

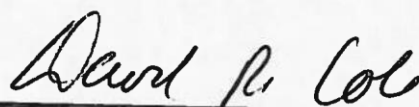
METHOD DEVELOPMENT  
FOR DISSOLVED INORGANIC AND ORGANIC CARBON ANALYSIS  
OF FLOWBACK FLUIDS FROM THE UTICA-POINT PLEASANT FORMATION

Undergraduate Research Thesis  
Submitted in partial fulfillment of the requirements for graduation  
with research distinction in Earth Sciences  
in the undergraduate colleges of  
The Ohio State University

By

Christina D. Jauregui  
The Ohio State University  
2017

Approved by

A handwritten signature in cursive script, reading "David R. Cole", is positioned above a horizontal line.

Dr. David R. Cole, Project Advisor  
School of Earth Sciences

## Table of Contents

Abstract .....	ii
Acknowledgements .....	iii
List of Figures .....	iv
List of Tables .....	v
1. Introduction .....	1
2. Geologic Setting .....	3
3. Methods .....	6
3.1 Laboratory Instruments .....	6
3.2 Raw Data Processing .....	9
3.3 Experimental solutions .....	10
3.3.1 Laboratory materials .....	10
3.3.2 DIC methodology .....	12
3.3.3 DOC methodology .....	13
3.4 Freshwater input and produced fluid sample collection .....	16
4. Results .....	17
4.1 DIC .....	17
4.1.1 OI Analytical Aurora (TICTOC) .....	17
4.1.2 Picarro CRDS .....	20
4.2 DOC .....	21
4.2.1 OI Analytical Aurora (TICTOC) .....	21
4.2.2 Picarro CRDS .....	27
4.3 Field Samples .....	30
Discussion .....	33
Conclusions .....	38
Recommendations for Future Work .....	40
References Cited .....	41
Appendices .....	43

## ABSTRACT

This research addresses rock-fluid interactions that occur between hydraulic fracturing fluids and shale formations to analyze geochemical reactions that occur in the subsurface. Specifically, the fractionation of  $^{13}\text{C}$  isotopes in dissolved inorganic carbon (DIC) and dissolved organic carbon (DOC) can be used as a tracer to determine carbon sources. Flowback fluids from the Utica-Point Pleasant in eastern Ohio have high salinity and complex chemistry, thus posing challenges for analysis. Experimental solutions and samples were analyzed for DIC, DOC, and  $\delta^{13}\text{C}$  using an OI Analytical Aurora Model 1030 Carbon Analyzer (TICTOC) interfaced with a Picarro Cavity Ring-Down Spectrometer (CRDS). Methods for measuring DIC, DOC and  $\delta^{13}\text{C}$  are developed to investigate and resolve chloride interference of high salinity brines and to determine effectiveness or limitations of wet chemical oxidation. Results of DIC analysis on experimental solutions that cover a range of salinity and DIC concentrations expected for flowback fluids show relatively stable  $\delta^{13}\text{C}$  signals when  $\text{CO}_2$  concentrations are high and that there is little fractionation in the  $\delta^{13}\text{C}$  signals over a range of salinity. However, results of DOC analysis affirm that elevated salinity inhibits the oxidation reaction thereby hindering  $\text{CO}_2$  recovery. DOC results from the CRDS data give stable  $\delta^{13}\text{C}$  signals when  $\text{CO}_2$  concentrations are high, but measured  $\delta^{13}\text{C}$  changes significantly as a function of chloride concentration in solution. Laboratory experiments explored various efforts to maximize  $\text{CO}_2$  recovery in the wet chemical oxidation process, which include (1) extending DIC/DOC reaction and detection times, (2) adjusting the addition of sodium persulfate, (3) variability of recovery in the presence of  $\text{NaCl}$  or  $\text{CaCl}_2$  salts, and (4) two organic compounds (potassium hydrogen phthalate and acetic acid) that differ in chemical structure.

## ACKNOWLEDGEMENTS

First and foremost, I would like to thank God. For with His grace and blessing, I have achieved a higher level of academic education and conducted this research study.

It is my pleasure to take this opportunity to sincerely thank my advisor Dr. David Cole, along with the members of the SEMCAL team, all of whom have challenged and assisted me in collaborating my ideas for developing this research. Thank you to Dr. Cole for taking me as an unexperienced undergraduate student and devoting his time to making me the successful researcher I am today. To Dr. Susan Welch, I would like to express my deepest appreciation for your encouragement, guidance, and training that made this research project possible. I would also like to thank Dr. Julie Sheets for your consistent and positive guidance in my research writing and undertakings. I would like to express my gratitude to Dr. Anne Carey for your influential guidance and encouragement during my undergraduate studies.

Thank you to Gulfport Energy for this research opportunity. Thank you for your cooperation with field sampling and providing samples for analysis discussed in this research thesis project.

I would like to thank all those involved with the essential financial funding I have received. Thank you to the Shell Exploration and Production Company for providing funding for my research through the Shell Undergraduate Research Experience (SURE) internship. My sincere gratitude is extended to the Willis E. “Bill” Rector Scholarship Awards. I hope to have made the Rector family very proud. I would like to personally thank Ms. Janie Rector for her enthusiastic encouragement throughout my research and education endeavors. My family and I have been greatly blessed through the Rector family’s support and we will always hold the Rector Family dear to our hearts. My sincere gratitude is extended to the School of Earth Sciences for the Willis E. “Bill” Rector Scholarship awarded to me. Lastly, I would like to thank the Critical Difference for Women Scholarship program for their significant and vital support for my entire journey here at The Ohio State University.

I would also like to give a huge “*THANK YOU*” to my family. To my four children, Alyssa, Makayla, Sadie, and Isabella, thank you for believing in your Mommy. We did it together! The sky is the limit my little ones, and as you continue to grow older, go and conquer your dreams and aspirations. I send a heartfelt thank you to my fiancé, Hunter. Thank you for believing in me, offering encouragement, and pushing me to stay motivated during this journey. You are my rock and I look forward to conquering the future with you. Thank you to my parents, Rodney and Linda. I am dearly blessed to be your daughter and to have received your enduring love. Thank you to my Aunt Wendy and Uncle Orlando for your continued support and encouragement. All of you are my inspiration and my academic success would not have been possible without your daily encouragement.

I would like to extend many thanks to all the Ohio State University School of Earth Science professors that have devoted themselves to teaching, training, and challenging me to explore my love of Earth Science. Thank you to all of my fellow Earth Science classmates for your collaboration, good humor, and friendship, especially during the late nights working and studying in Mendenhall. You have all made this journey truly memorable.

## LIST OF FIGURES

1. Early Late Ordovician strata
2. TOC map
3. TICTOC schematic diagram
4. CRDS schematic diagram
5. “Sniff and Pulse” peaks
6. KHP and acetic acid structures
7. Sampling location
8. DIC instrument calibration data
9. Extending DIC reaction and detection times
10. DIC salt control data
11. DIC  $\delta^{13}\text{C}$  data
12. Extending DIC reaction and detection times
13. 10ppm DOC salt control data
14. DOC salt control data
15. 10ppm DOC with NaCl and CaCl<sub>2</sub> data
16. Oxidizing reagent volume and 10ppm DOC 10g/L NaCl data
17. Oxidizing reagent volume data
18. DOC  $\delta^{13}\text{C}$  data
19. KHP and acetic acid [DOC] and  $\delta^{13}\text{C}$  data
20. Field sample [DIC] overtime
21. Field sample [DIC]
22. Field sample  $\delta^{13}\text{C}$  data overtime
23. Field sample [DOC] and  $\delta^{13}\text{C}$  data
24. Flowback [DOC] and  $\delta^{13}\text{C}$  data

## **LIST OF TABLES**

1. Total vertical depth (TVD)
2. Formation depths
3. DIC stock solutions.
4. Method conditions used in TICTOC procedures

## **1. INTRODUCTION**

With continued growth of hydraulic fracturing within the Utica-Point Pleasant shale gas reservoirs of eastern Ohio, efforts have increased to analyze quantity and chemistry of produced fluids. Produced fluids are waters that have circulated in the subsurface and then flowed back through the well borehole returning to the surface. Developing hydraulic fracturing wells requires a tremendous volume of water, which involves pumping thousands of barrels of water into rock formations at high pressures (Wattenbarger and Alkouh, 2013). Hydraulic fracturing wells are developed in stages and flowback fluids contain complex chemistry depending on well development and production stages (King, 2012). Waters introduced into a shale formation typically remain in the subsurface, because under-saturated shale clay matrixes trap water within small pores, until returning back to the surface during well production stages. Many hydraulic fracturing wells are developed by using freshwater sources, but in some areas of Ohio it is becoming more common to reuse flowback fluids (Kondash et al., 2017). In order to evaluate the complex chemistry of hydraulic fracturing fluids coming out of wells, this research project not only implements steps to analyze flowback fluids, but also to analyze the chemistry of fresh water that is introduced to the wells. Flowback fluids have high salinity with research suggesting elevated salinity is due to the dissolution of salts present within the formation or by the interaction with basinal brines (Vazquez et al., 2014).

Carbon geochemistry of flowback fluids is relevant to understanding water-rock interactions occurring between hydraulic fracturing flowback fluids and shale formations. The research reported on herein focuses on developing analytical methods to measure concentrations and isotopic compositions of dissolved inorganic carbon (DIC) and dissolved organic carbon (DOC) from hydraulic fracturing flowback fluids interacting with the Utica-Point pleasant



formation of eastern Ohio. Carbon isotopic signatures are used as tracers that can enhance our understanding of interactions occurring between hydraulic fracturing fluids and shale formations in the subsurface. Measurements of  $^{12}\text{C}/^{13}\text{C}$  ratios are obtained by analyzing carbon dioxide ( $\text{CO}_2$ ) gas, resulting from the acidification of DIC or oxidization of DOC in aqueous solutions using a carbon analyzer instrument, using a cavity ring down laser absorption spectrometry technique. When recovered  $\text{CO}_2$  concentrations are low, optimal  $^{12}\text{C}/^{13}\text{C}$  ratio measurements can be hindered, thus emphasizing importance of maximizing recovery of  $\text{CO}_2$ . In this study, method developments focused on maximizing  $\text{CO}_2$  recovery during acidification of DIC and wet chemical oxidation (WCO) of DOC for brine solutions in order to determine  $\delta^{13}\text{C}$  composition. Evolution of  $\text{CO}_2$  from the acidification of DIC is more direct and less complicated than WCO of DOC. WCO techniques used for measuring DOC are more difficult due to chemical interference of DOC oxidation in saline waters (McKenna and Doering, 1995). Measuring DOC has developed much controversy and critical review (Wangersky, 1993), thus prompting consideration of new studies (such as ours) to improve the efficiency of WCO-DOC techniques.

## 2. GEOLOGIC SETTING

The Upper Ordovician in eastern Ohio has attracted attention as a major unconventional hydrocarbon producing interval, specifically due to the Point Pleasant Formation's considerable hydrocarbon generation. Subsurface units of this region include formations (Figure 1) that were deposited in a shallow marine environment with the accumulation of carbonates on a carbonate platform during building up sequence events (McClain, 2012). Frequent storms greatly affected the depositional environment, indicating the accumulation of sediments that were influenced by shallow waters with high energy conditions (Smith, 2014).

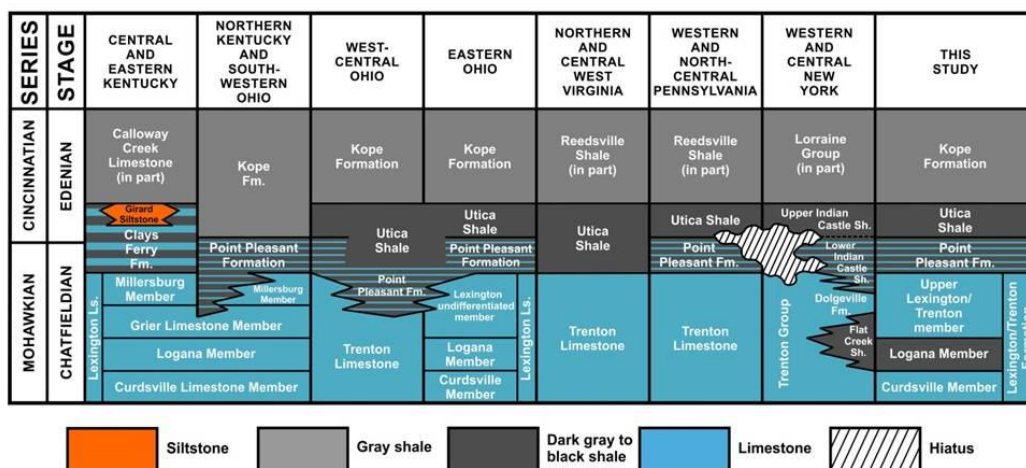


Figure 1. Early Late Ordovician strata (Utica Shale Play Book Study, Hickman et al., 2015a).

The Utica Shale Formation contains varying thicknesses of interbedded fissile shale to calcareous shale beds resulting from eustacy and basinal tectonics events (Hickman et al., 2015b). TOC concentrations of the Utica Shale range from 0.5% to 3.3%, with the highest measured TOC developed toward the Eastern Ohio area (Harrington et al., 2013). The Point Pleasant Formation, a gray shale including coarse limestone storm beds, contains an upper section which is organically poor (TOC <1%) with carbonate content ranging from 25% to 50%, along with a lower section that is organically rich (up to TOC of 5%) and carbonate content

ranging from 40% to 60% (Hickman et al., 2015a). The thickness of the Point Pleasant Formation ranges from 0 to 240 feet across Ohio into Pennsylvania. The concentration of organic matter across Ohio increases in the eastward direction (Figure 2).

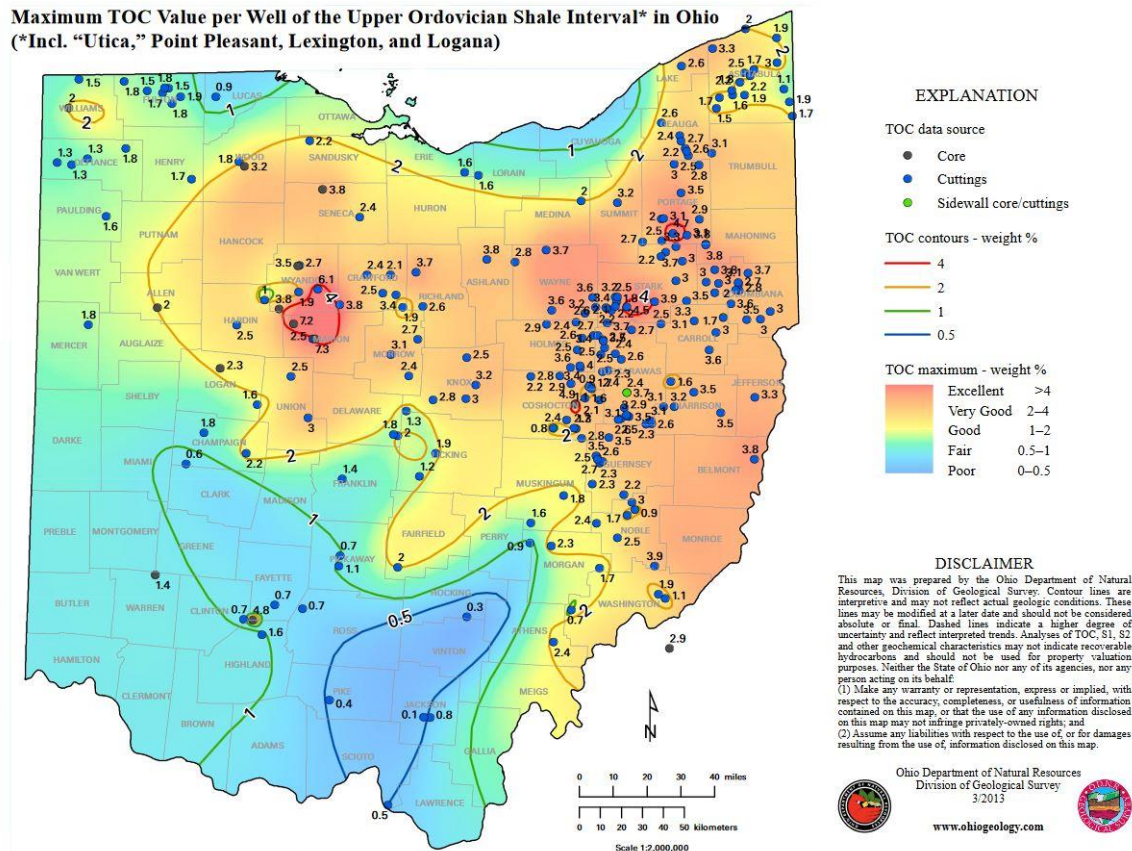


Figure 2. Ohio Department of Natural Resources, Division of Geologic Survey's map of maximum TOC concentrations measured from the Upper Ordovician Shale Interval. TOC concentrations increase progressing eastward. (ODNR, 2013).

According to Actual Well Reports and Well Completion Records retrieved from the Ohio Oil and Gas Well Database, drilling completion depths for all four Eastern Ohio wells (U/PtP-1 through U/PtP-4) studied in this research targeted the Point Pleasant Formation (Tables 1 and 2).

Table 1. Total vertical depth (TVD) (ft) and Driller's total depth (TD) (ft) measurements acquired from Well Completion Records for wells U/PtP-1 through U/PtP-4. Retrieved from Ohio Oil and Gas Well Database ([apps.ohiodnr.gov/oilgas/rbdmsreports/](https://apps.ohiodnr.gov/oilgas/rbdmsreports/)).

Well	Total Vertical Depth (ft)	Driller's Total Depth (TD) (ft)
U/PtP-1	9739.89	16165
U/PtP-2	9745.91	16809
U/PtP-3	9758.25	16814
U/PtP-4	9751.88	17704

Table 2. Formation depth measurements from Actual Well Reports for wells U/PtP-1 through U/PtP-4. Reports retrieved from Ohio Oil and Gas Well Database ([apps.ohiodnr.gov/oilgas/rbdmsreports/](https://apps.ohiodnr.gov/oilgas/rbdmsreports/)).

		Well Identification			
		U/PtP-1	U/PtP-2	U/PtP-3	U/PtP-4
Top of Formation Depths (ft)	Big Lime	5595	5571	5571	5566
	Oriskany	5778	5750	5750	5756
	Salina	6156	6144	6144	6156
	Parker Shell	7606	7672	7672	7666
	Queenston	7936	7910	7910	7840
	Utica	8972	8077	8077	8930
	Point Pleasant	9561	9565	9565	9567

### 3. METHODS

#### 3.1 Laboratory Instruments

Experimental solutions and natural samples were analyzed using an OI Analytical Aurora Model 1030 Carbon Analyzer (TICTOC) interfaced to a Picarro Cavity Ring-down Spectrometer (CRDS) located in Subsurface Energy Materials Characterization and Analysis Lab (SEMCAL) at The Ohio State University School of Earth Science.

TICTOC aqueous reagents were used to evolve CO<sub>2</sub> through complete acidification of DIC and/or complete oxidation of DOC in a reaction chamber. Total inorganic carbon (TIC) and total organic carbon (TOC) concentrations from evolved CO<sub>2</sub> is measured by the non-dispersive infrared (NDIR) detector. After NDIR measurements are completed, collected CO<sub>2</sub> gas is then stored within a gas-tight bag until it is introduced into the CRDS cavity for subsequent analysis of carbon isotopes. A schematic setup of the TICTOC instrument is shown in Figure 3, along with details of key steps. The TICTOC and CRDS setup is similar to that used by Conaway et al. (2015), except their experimental procedures used nitrogen (N<sub>2</sub>) as a carrier gas, while our system uses oxygen (O<sub>2</sub>).

Experimental DIC (sodium bicarbonate) solutions and natural freshwater samples were acidified in the reaction chamber with 5% phosphoric acid to evolve CO<sub>2</sub> from the DIC that is subsequently measured by the NDIR. The general chemical reaction for acidification of DIC by phosphoric acid is as follows:



Experimental DOC (KHP and acetic acid) solutions were initially reacted with 5% phosphoric acid reagent in the reaction chamber to acidify the sample in order to purge all DIC and CO<sub>2</sub> from the system. Then, 10% sodium persulfate reagent is introduced into the reaction

chamber which is heated to 98°C to complete oxidation of DOC, which in turn evolves CO<sub>2</sub> that is measured with the NDIR. The general chemical reaction during wet chemical oxidation (WCO) of DOC by persulfate chemistry is as follows:

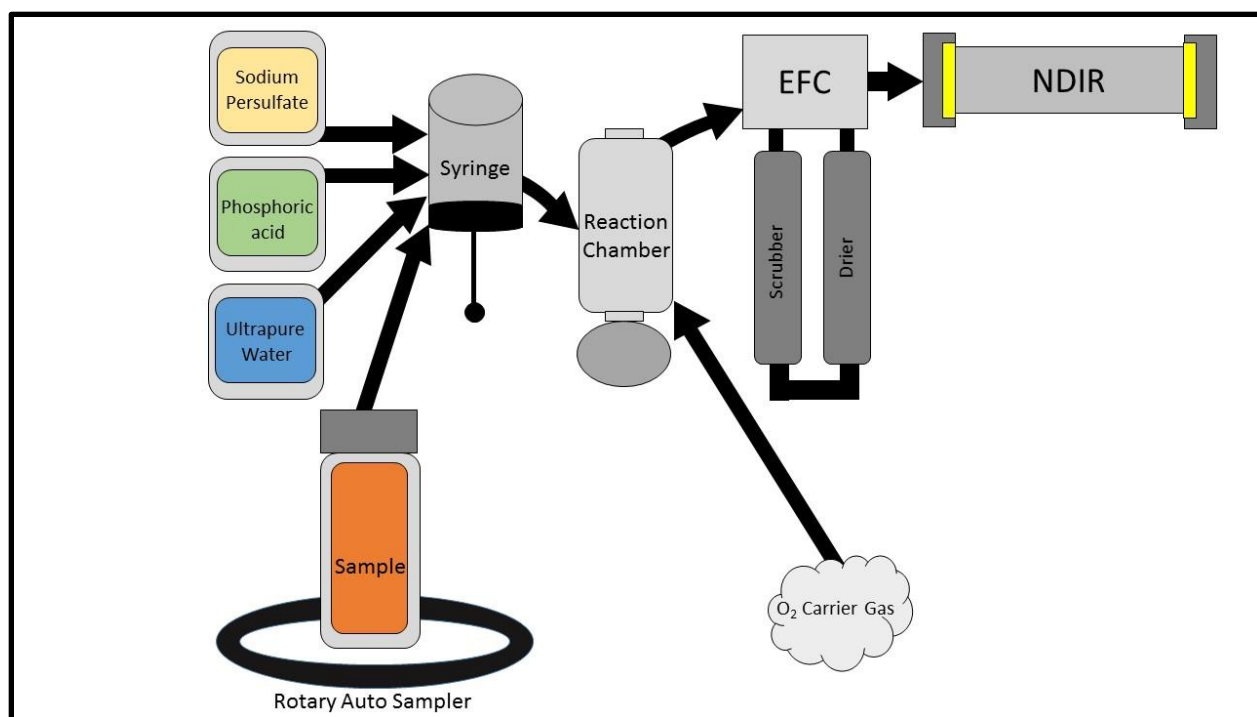
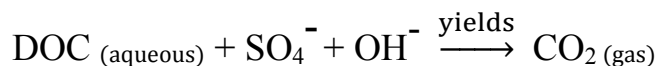
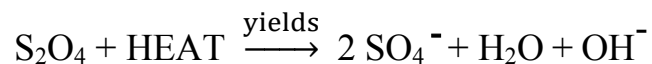


Figure 3. Schematic diagram of WCO configuration used to analyze experiments. Schematic is similar is to Conaway et al. (2015).

After acidification of DIC and WCO of DOC are completed, the CO<sub>2</sub> gas from the gas-tight bag enters into the cavity-ring down spectrometer for  $\delta^{13}\text{C}$  composition measurements. In the CRDS cavity (Figure 4), CO<sub>2</sub> molecules absorb light from a beam from a single-frequency laser diode. A photodetector detects light intensity signals and measures the decay “ring down” of light intensities exponentially. In turn, molar fractions of trace gas constituents can be

determined from the decaying light intensity bouncing back on forth between the mirrors. Therefore,  $\delta^{13}\text{C}$  compositions can be obtained. Carbon isotopic compositions are reported relative to the international PDB (Pee Dee Belemnite) standard, which yield  $\delta^{13}\text{C}$  compositions as a positive or negative value. A positive  $\delta^{13}\text{C}$  value indicates that the isotopic ratio of the sample is higher relative to the PDB standard value, while a negative  $\delta^{13}\text{C}$  value indicates that the isotopic ratio is lower than the PDB standard (Kendall, 1999).

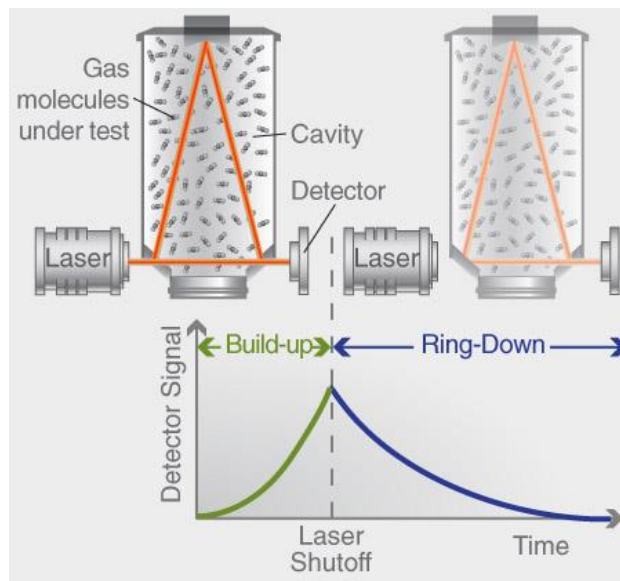


Figure 4. Schematic of Picarro CRDS analyzer showing how ring down measurement is carried out ([www.picarro.com](http://www.picarro.com)).

### 3.2 Raw Data Processing

Measurements from TICTOC reports were retrieved and used in this study that provided time integrated CO<sub>2</sub> measurements along with important details (i.e. system parameters) for each analyzed sample.  $\delta^{13}\text{C}$  isotopic compositions were calculated similar to the Hartland et al. study (2012). Data processing methods focused on analyzing UserLog.dat data files retrieved from CRDS system's time-integrated measurements. This required extensive “hand” processing of data files to identify two separate measurement peak values for all experimental solutions. More explicitly, by identifying two measurement peaks correlating to each analysis we could identify the first peak as characteristically small (referred to as the “sniff”), which the instrument software uses to determine CO<sub>2</sub> concentration in the gas, followed by a larger, extended second peak (referred to as the “pulse”) used to determine isotopic composition (Figure 5).

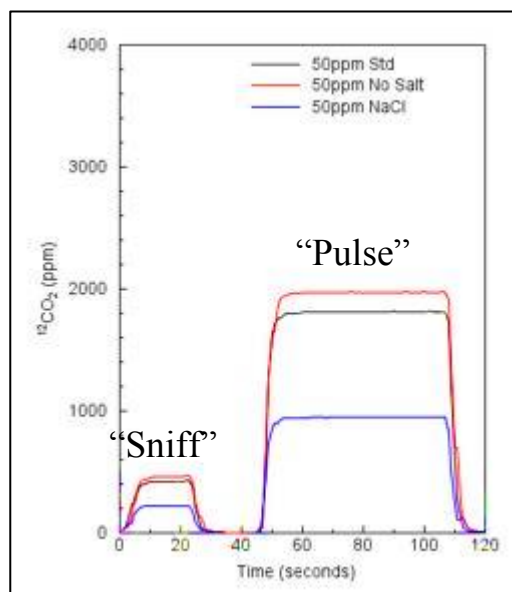


Figure 5. Two peaks (“sniff” and “pulse”) filtered from CRDS logs.



### 3.3 Experimental solutions

#### 3.3.1 Laboratory materials

Instrument calibration and experimental solutions were created using reagent grade chemicals and ultrapure (Mill-Q™) waters. The instrument system reagents (ultrapure water/18 M-Ohm water, 5% phosphoric acid solution, and 10% sodium persulfate solution) were stored in plastic bottles connecting to the reaction chamber that allows reagent volume (via syringe) to be introduced into the chamber (Figure 3). Phosphoric acid reagents were made by adding 50 ml reagent grade phosphoric acid to 1 liter of water. Sodium persulfate reagents were made by adding 100 grams reagent grade sodium persulfate to 1 liter of water.

Test solutions for DIC method development were prepared using reagent grade sodium bicarbonate ( $\text{NaHCO}_3$ ). Three stock solutions of 1000 mg/L C as  $\text{NaHCO}_3$  were prepared using sodium bicarbonate powder with different carbon isotopic compositions and ultrapure water in new amber bottles that were rinsed with ultrapure water before use. The first stock solution was prepared by diluting 3.497 grams  $\text{NaHCO}_3$  ( $\delta^{13}\text{C}$  -2‰) in 494.3 ml of ultrapure water. The second stock solution was prepared by diluting 3.499 grams  $\text{NaHCO}_3$  ( $\delta^{13}\text{C}$  -14‰) to 493.2 ml of ultrapure water. The final stock solution was prepared by diluting 3.500 grams  $\text{NaHCO}_3$  ( $\delta^{13}\text{C}$  -18‰) in 493.26 ml of ultrapure water. Finally, all these 1000 g/L C as  $\text{NaHCO}_3$  stock solutions were then used to prepare four additional lower concentration standard solutions in new amber bottles that had been rinsed with ultrapure water before use (Table 3).

Table 3. DIC stock solutions.

DIC STOCK SOLUTIONS				
NaHCO <sub>3</sub> [Stock solution] (ppm)	$\delta^{13}\text{C}$ (‰)	1000 ppm NaHCO <sub>3</sub> (aq) (ml)	Ultrapure Water (ml)	Total weight
10	-2	1.99	198.00	199.99
20		3.97	196.07	200.04
50		9.99	190.01	200.00
100		19.99	180.26	200.25
10	-14	1.98	198.01	199.99
20		4.00	196.05	200.05
50		9.97	190.10	200.07
100		19.99	180.15	200.14
10	-18	2.00	198.00	200.00
20		4.00	196.02	200.02
50		9.98	190.02	200.00
100		19.98	180.07	200.05

Preparation of DOC experimental solutions involved using reagent grade potassium hydrogen phthalate “KHP” (C<sub>8</sub>H<sub>5</sub>KO<sub>2</sub>) and acetic acid (C<sub>2</sub>H<sub>4</sub>O<sub>2</sub>) solutions for preparing 1000 ppm C stock solutions. Additional test solutions were prepared with NaCl and CaCl<sub>2</sub> concentrations to simulate complex chemistry typically existing in flowback fluids. A 200 ml solution of 1000 mg/L KHP stock solution was prepared by diluting 0.43 grams of KHP powder with 199.62 ml of ultrapure water in a new amber bottle that was rinsed with ultrapure water before use. The 1000 mg/L KHP stock solution was then used to prepare four additional 200 ml KHP stock solutions (at lower concentrations) in new amber bottles that had been rinsed with ultrapure water before use. The four additional KHP stock solution concentration included; 1ppm

KHP solution (0.4 ml of 1000 mg/L KHP with 199.61 ml ultrapure water), 5ppm KHP solution (0.99 ml of 1000 mg/L KHP with 199.22 ml ultrapure water), 10ppm KHP solution (1.99 ml 1000 mg/L of KHP with 198.06 ml ultrapure water), and a 50ppm KHP stock solution (10 ml of 1000 mg/L KHP with 190.29 ml ultrapure water). For our additional DOC standard solutions, a 10ppm acetic acid stock solution was prepared by diluting 0.42 ml of reagent grade 1.0 N acetic acid solution in 999.58 ml of ultrapure water.

Salt solutions added to DIC/DOC stock solutions were prepared to test the effects of elevated salinity on the analytical methods. To prepare a 200g/L sodium chloride (NaCl) stock solution, new plastic bottles were first rinsed with ultrapure water and then used to dissolve reagent grade NaCl crystals in ultrapure water. The calcium chloride (CaCl<sub>2</sub>) stock solution was prepared by dissolving 62.81 grams of reagent grade CaCl<sub>2</sub> · 6 H<sub>2</sub>O with 250 ml of ultrapure water.

### 3.3.2 DIC methodology

*DIC Experiment #1.* Experimental sodium bicarbonate solutions with three different  $\delta^{13}\text{C}$  compositions of -2, -14, and -18 ‰ were transferred into clean 40 ml glass vials and then placed into the instrument auto sampler (Figure 3). The evolved CO<sub>2</sub> resulting from acidification of DIC was collected to measure DIC concentrations. Collected CO<sub>2</sub> gas was then sent to the CRDS for  $\delta^{13}\text{C}$  composition measurements. Key conditions pertaining to DIC Experiment #1 are listed in Table 4.

*DIC Experiment #2.* Experiment #2 involved using sodium bicarbonate solutions at varied concentrations containing 200 g/L NaCl salinity concentrations to simulate typical subsurface brines and investigate the possible effects of chloride on the DIC concentration and isotopic analysis. Sodium bicarbonate solutions and 200 g/L NaCl solutions were pipetted into

clean 40 ml glass vials and then placed into the instrument auto sampler. Method development also included extending DIC reaction times from 1.5 minutes to 2.0 minutes and DIC detection times from 3.0 minutes to 4.0 minutes to optimize CO<sub>2</sub> recovery. The evolved CO<sub>2</sub> resulting from acidification was collected to measure DIC concentrations before finally sending CO<sub>2</sub> gas to the CRDS for  $\delta^{13}\text{C}$  composition measurements. Key conditions pertaining to DIC Experiment #2 are given in Table 4.

### 3.3.3 DOC methodology

*DOC Experiment #1.* The first DOC method involved running a standard curve for KHP experimental solutions over a range of concentrations. After first purging DIC from the sample, WCO then proceeds to oxidize DOC to evolve CO<sub>2</sub> at DOC reaction time of 2.5 minutes and DOC detection time of 4.5 minutes for DOC concentration measurement. The collected CO<sub>2</sub> gas is sent to the CRDS for  $\delta^{13}\text{C}$  composition measurements. Key conditions pertaining to DOC Experiment #1 are displayed in Table 4.

*DOC Experiment #2.* The method approach for Experiment #2 further investigated the effect of chloride interference during WCO. To investigate chloride interference, 1ppm, 10ppm, and, 50 ppm KHP stock solutions were combined with NaCl or CaCl<sub>2</sub> salt solutions over a range of Cl<sup>-</sup>. KHP standard solutions and NaCl and CaCl<sub>2</sub> salt solutions were pipetted into clean 40 ml glass vials and placed into the instrument's auto sampler. A second key method development within Experiment #2 was to increase reaction and detection times compared to Experiment #1, which involved increasing DOC reaction time to 3.5 minutes and DOC detection time to 6.5 minutes. The evolved CO<sub>2</sub> resulting from WCO was collected and measured for DOC concentrations before being sent to the CRDS for  $\delta^{13}\text{C}$  measurements. Key conditions pertaining to DOC Experiment #2 are listed in Table 4.

*DOC Experiment #3.* DOC method approach for Experiment #3 included adjustment to the volume of sodium persulfate injected during the WCO process. 10 ppm KHP and 10ppm acetate solutions with a range of salinities were prepared and transferred into clean 40 ml glass vials. Experimental solutions were then reacted with 2 ml or 4 ml of sodium persulfate reagent solution to optimize the oxidation of DOC. The evolved CO<sub>2</sub> resulting from WCO was collected to measure DOC concentrations. Finally, the CO<sub>2</sub> gas was sent to the CRDS for  $\delta^{13}\text{C}$  composition measurements. Key conditions pertaining to DOC Experiment #3 are given in Table 4.

*DOC Experiment #4.* Method development proceeded to investigate WCO of acetic acid (Figure 6). Although KHP is a commonly used DOC standard in laboratory analysis, ion chromatography detected acetic acid to be the most abundant carboxylic acid measured in the hydraulic fracturing flowback fluids (approximately ~50ppm) and is abundant in oilfield brines. 10 ppm C as acetate solutions with a range of Cl<sup>-</sup> concentrations were prepared by pipetting acetate, NaCl, or CaCl<sub>2</sub> solutions into clean 40 ml glass vials which were then placed into the instruments auto sampler. The evolved CO<sub>2</sub> resulting from WCO was measured by the NDIR to determine DOC concentrations. Finally, the CO<sub>2</sub> gas was sent to the CRDS for  $\delta^{13}\text{C}$  composition measurements. Key conditions pertaining to DOC Experiment #4 are listed in Table 4.

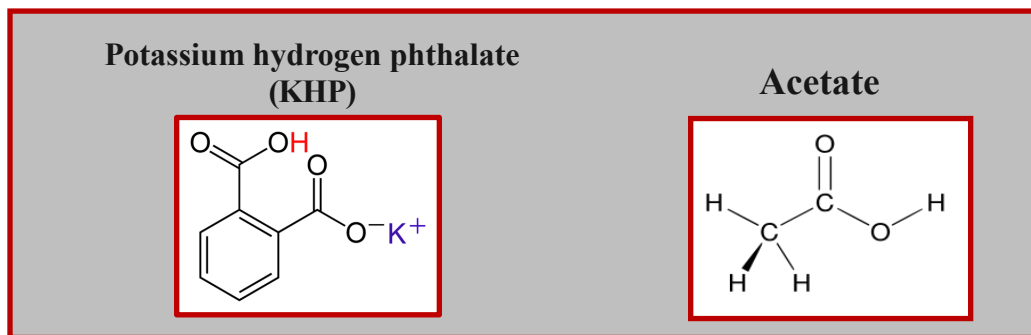


Figure 6. Molecular structures of potassium hydrogen phthalate (KHP) and acetate. KHP consists of complex carbon bonds more difficult to break during chemical oxidation, while acetate is composed of single carbon bonds which chemical oxidation can easily liberate into evolved CO<sub>2</sub> gas.

Table 4. Method conditions used in TICTOC procedures.

DIC and DOC Method Parameters						
Key Parameter	DIC Experiment 1	DIC Experiment 2	DOC Experiment 1	DOC Experiment 2	DOC Experiment 3	DOC Experiment 4
Sample	NaHCO <sub>3(aq)</sub>	NaHCO <sub>3(aq)</sub>	KHP	KHP	KHP Acetic acid	KHP Acetic acid
Sample [con] (ppm)	10, 20, 50, 100	10, 20, 50, 100	1, 10, 50	1, 10, 50	1, 5, 10, 50	10
Sample volume (ml)	8	5	5	5	5	5
Salt	_____	NaCl	_____	NaCl, CaCl <sub>2</sub>	NaCl, CaCl <sub>2</sub>	NaCl, CaCl <sub>2</sub>
Salt Concentration s (g/L)	_____	200	_____	0, 1, 5, 10, 20	0, 1, 5, 10, 20	0, 1, 5, 10, 20
5% H <sub>3</sub> PO <sub>4</sub> volume (ml)	0.5	1.0	1.0	1.0	1.0	1.0
10% Na <sub>2</sub> S <sub>2</sub> O <sub>8</sub> volume (ml)	_____	_____	2.0	2.0	2.0 4.0	2.0 4.0
DIC Reaction time (mins)	1.5	2.0	1.5	2.0	2.0	2.0
DIC Detection time (mins)	3.0	4.0	3.0	4.0	4.0	4.0
DOC Reaction time (mins)	_____	_____	2.5	3.5	3.5	3.5
DOC Detection time (mins)	_____	_____	4.5	6.5	6.5	6.5
Replicates	3	3	2	2	2	2

### 3.4 Freshwater input and produced fluid sample collection

Freshwater input and produced fluid samples were collected at a hydraulic fracturing site located in eastern Ohio, Monroe County (Figure 7). Freshwater input samples were collected every two weeks between April 2015 and May 2015. Produced fluid samples were collected several times from July 2015 through November 2015. Freshwater samples analyzed in this study were collected from a freshwater holding tank on the well pad and a nearby pond which was one source of the fresh water. Hydraulic fracturing flowback or produced fluids were collected from four actively producing wells on the well pad. Flowback fluids were collected from fluid tanks situated at each of the four wells. Company personnel collected samples of flowback fluids from the separators in 10 liter carboys which were quickly subsampled and filtered in the field for various analysis by Ohio State personnel. Samples for DIC and DOC analysis were unfiltered and were stored in the refrigerator until analyzed.



Figure 7. Red star indicates the field site location where samples were collected in Monroe County, Ohio.

## 4. RESULTS

In order to develop methods to measure DIC, DOC, and carbon isotope ratios using the TICTOC-CRDS system, we had to analyze experimental solutions that contained a range of carbon concentrations, composition, salinity, and isotope composition. The efficiency of the methods was analyzed using data output from the NDIR detector on the TICTOC to determine the total carbon content evolved from solution (both timing and concentration) and then the signal measured by the CRDS to determine total carbon and carbon isotope ratios.

### 4.1 DIC

#### 4.1.1 OI Analytical Aurora (TICTOC)

Figure 8 shows results for analyzed DIC standard solution analysis and confirmed the effectiveness of the instrument for measuring DIC. CO<sub>2</sub> concentrations for DIC solutions are reproducible for all three replicates of each sample. Results show that measured CO<sub>2</sub> concentrations increase with increasing DIC concentration.

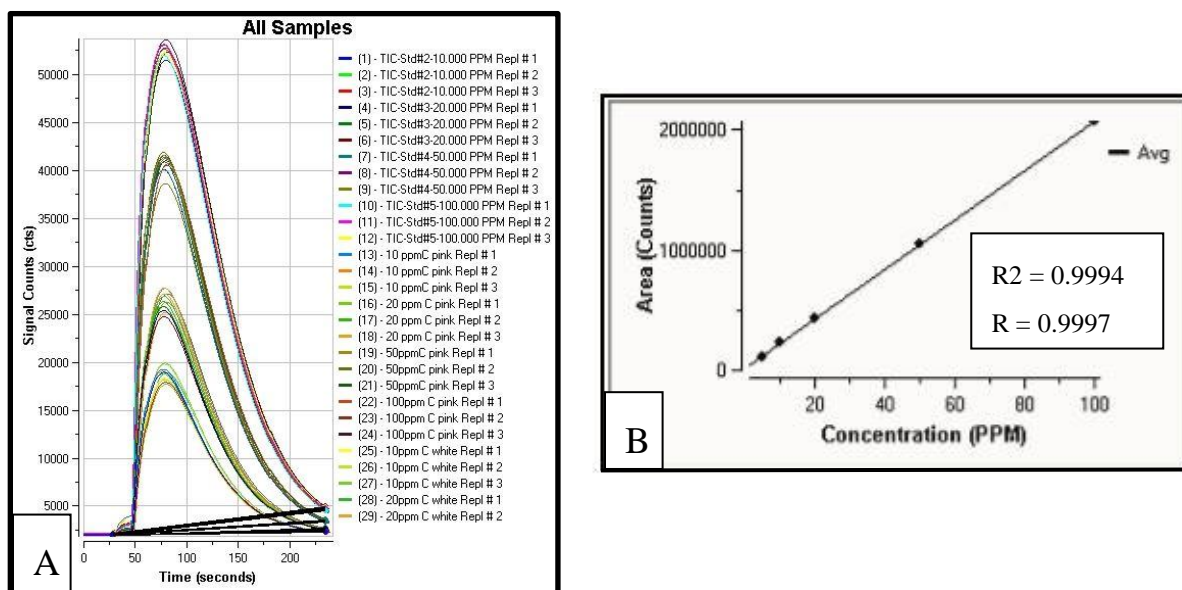


Figure 8. DIC calibration solutions compared to DIC standard stock solutions. A) DIC data showing CO<sub>2</sub> measurements including B) the calibration curve.



To improve DIC methods for analysis solutions, the times for both reaction and detection were extended. Initial DIC experimental solutions were tested with instrument parameters set for a reaction time of 1.5 minutes and detection time of 3 minutes, which produced incomplete CO<sub>2</sub> concentration curves (Figure 9A). Hence, by increasing DIC reaction time to 2 minutes and DIC detection time to 4 minutes, CO<sub>2</sub> recovery improved and allowed for more complete integration of signal counts (Figure 9B).

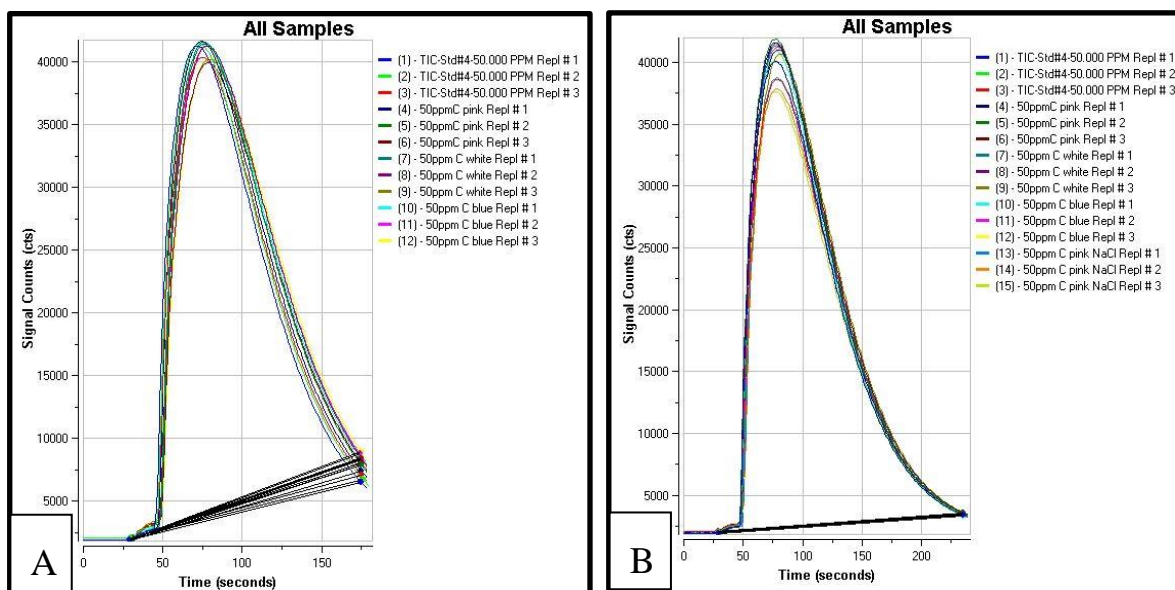


Figure 9. Data presents variability in the integration of signal counts. A) Figure A shows curves collected with DIC detection times set at 3.0 minutes that appear incomplete. B) Figure B shows extended DIC detection times increased to 4.0 minutes, which improved the integration of signal count and developed CO<sub>2</sub> concentration curves that are more complete.

Total CO<sub>2</sub> recovery from experimental solutions containing various DIC (NaHCO<sub>3</sub>) concentrations with 200 g/L NaCl were determined by analyzing the signal measured from the NDIR detector on the TICTOC (Figure 10). Data from the NIDR detector show that the evolution of CO<sub>2</sub> in salt free control and salty standard solutions are similar. Data show CO<sub>2</sub> concentration curves for DIC solutions containing 200 g/L NaCl are slightly smaller than the standards of DIC containing no salt, and we attributed the greater area under the curves of salt free control solutions are due to NaCl occupying volume of the salt standard solutions.

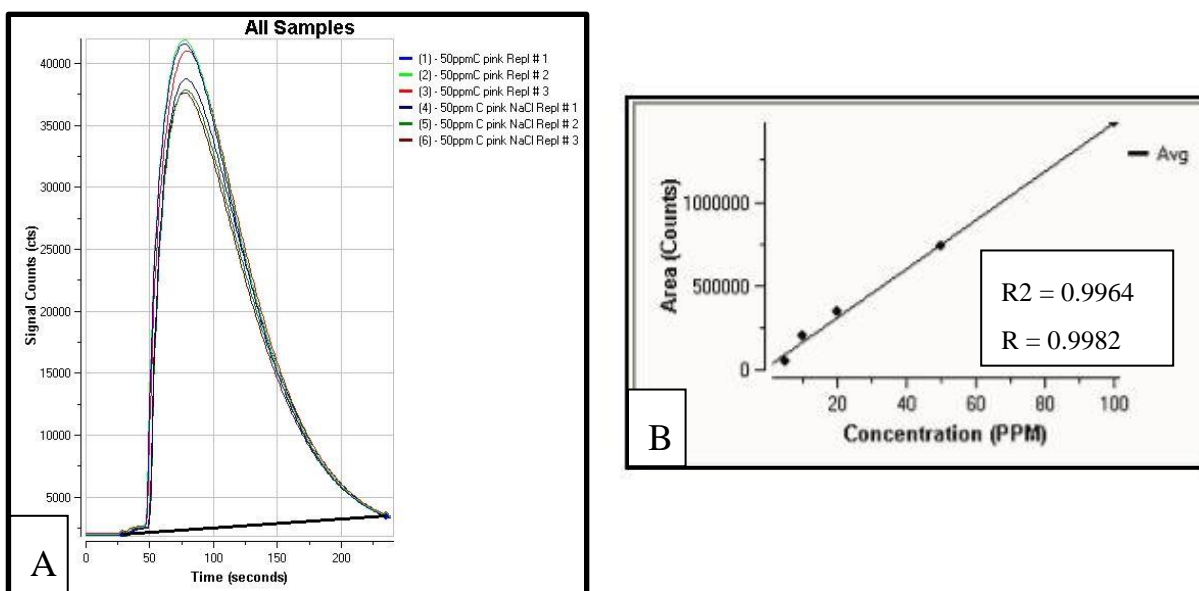


Figure 10. DIC no salt control solutions compared to DIC NaCl control solutions. A) DIC data showing CO<sub>2</sub> measurements including B) the calibration curve.

#### 4.1.2 Picarro CRDS

$\delta^{13}\text{C}$  concentration measurements for DIC ( $\text{NaHCO}_3$ ) solutions, as a function of concentration, with 200 g/L NaCl, were calculated from CRDS data logs and measurements show that  $\delta^{13}\text{C}$  signals of DIC for salt free control solutions are similar to those of high salt standards (Figure 11). For example, analysis for a solution of 100ppm DIC with  $\delta^{13}\text{C}$  of approximately -18 ‰ shows an averaged pulse peak  $\delta^{13}\text{C}$  signal value of  $-20.17 \pm 0.89$  compared to the 100ppm DIC ( $\delta^{13}\text{C}$  -18‰) 200 g/L NaCl solution with an averaged pulse peak  $\delta^{13}\text{C}$  signal value of  $-20.53 \pm 0.82$ . As DIC ( $\delta^{13}\text{C}$  -18‰) concentrations decrease, the averaged pulse peak  $\delta^{13}\text{C}$  signal value display greater variability, as shown by comparing 10ppm DIC ( $\delta^{13}\text{C}$  -18‰) solution with an averaged pulse peak  $\delta^{13}\text{C}$  signal value of  $-19.97 \pm 0.82$  compared to the 10ppm DIC ( $\delta^{13}\text{C}$  -18‰) 200 g/L NaCl solution with an averaged pulse peak  $\delta^{13}\text{C}$  signal value of  $-21.68 \pm 1.09$ . The results of this analysis clearly show that low DIC concentrated solutions evolve lower  $\text{CO}_2$  concentrations, therefore consequential  $\delta^{13}\text{C}$  signals are more variable while increased  $\text{CO}_2$  concentrations yield  $\delta^{13}\text{C}$  signals that become more reproducible.

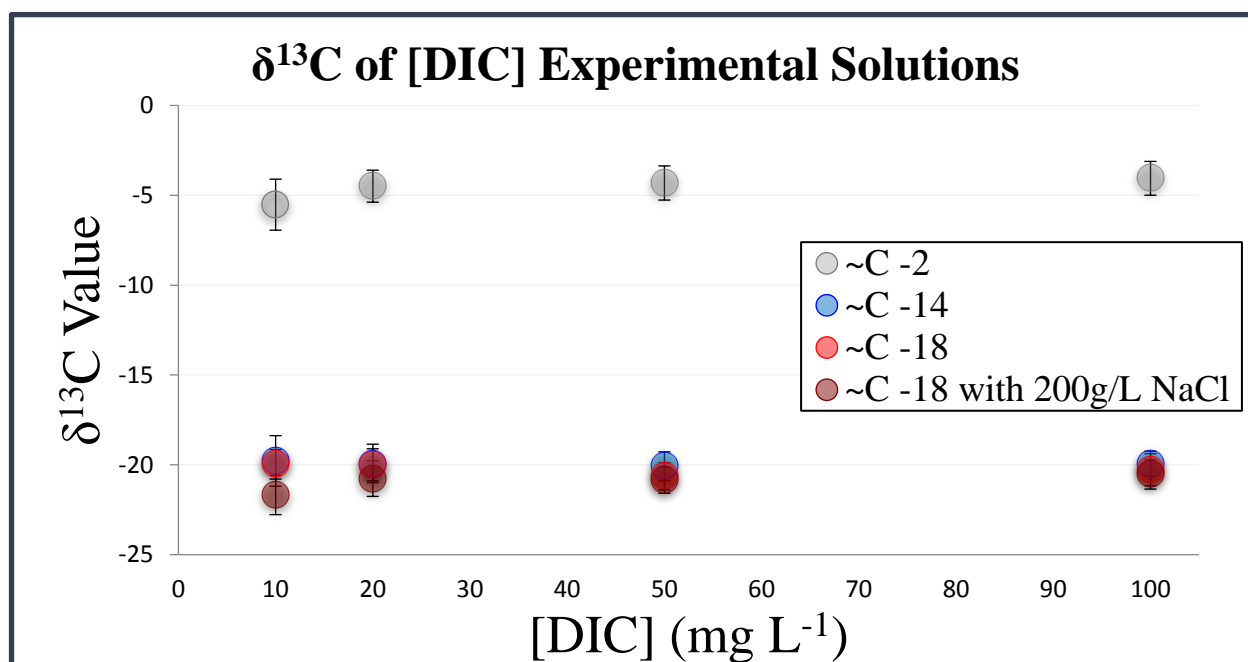


Figure 11. CRDS data of  $\delta^{13}\text{C}$  signal of DIC experimental solutions retrieved and analyzed from TICTOC-CRDS data logs.

## 4.2 DOC

### 4.2.1 OI Analytical Aurora (TICTOC)

Similar to DIC method development, DOC methods development began by adjusting the system's DOC reaction and detection (purge) times to improve complete oxidation and recover maximum CO<sub>2</sub> concentrations. Adjustment within this method development was similar to approaches implemented during Conaway et al. (2015) experiments, which used WCO conditions for DOC reaction time set to 3.0 minutes and DOC detection time set at 6.0 minutes. Initial experiments used WCO conditions (referenced as Method A) assigned DOC reaction time set at 2.5 minutes and DOC detection time set at 4.5 minutes. Results for Method A show that a 1ppm DOC 10 g/L NaCl solution gives a DOC area count of 18,308 by averaging two sample replicates. In Method B, which extended DOC reaction time to 3.5 minutes and DOC detection time set at 6.5 minutes, results show that a 1ppm DOC 10 g/L NaCl solution gives a DOC area count of 24,230 by averaging two sample replicates, which suggests Method B achieved more complete oxidation and significantly increased CO<sub>2</sub> recovery compared to Method A (Figure 12).

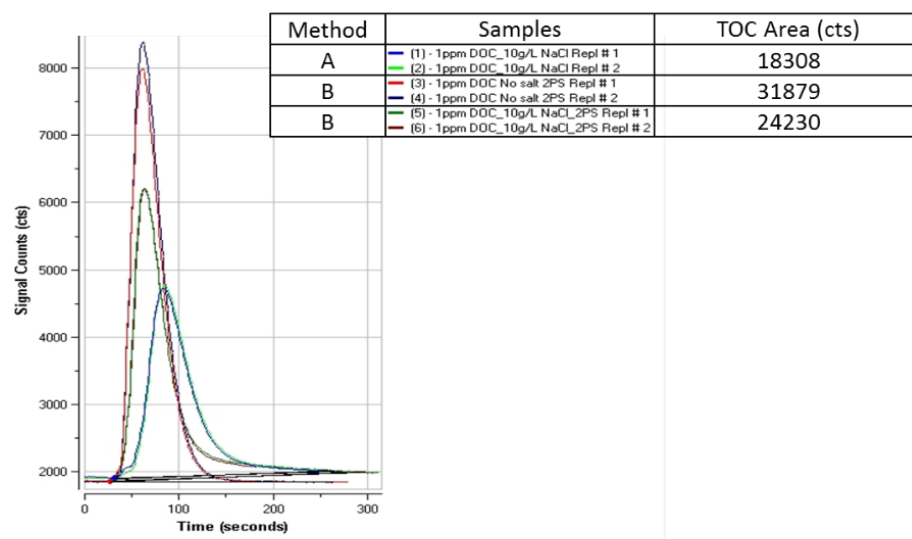


Figure 12. Method A and Method B results for extending DOC reaction time and detection time retrieved from OI Analytical Aurora (TICTOC) reports.

Total CO<sub>2</sub> recovery measurements for DOC solutions, as a function of concentration and salinity, show that increasing the chloride concentration resulted in decreased CO<sub>2</sub> recovery. DOC experimental solution containing 20 g/L CaCl<sub>2</sub> compared to no salt control solutions resulted in a decrease in CO<sub>2</sub> of approximately 50% in the presence of chloride (Figure 13). Similarly, additional DOC solutions (1ppm, 10ppm, and 50ppm) containing various concentrations of NaCl solutions also showed decreasing CO<sub>2</sub> recovery as salinity increased, thus demonstrating that CO<sub>2</sub> recovery is dependent on chloride concentration (Figure 14). Data shown in Figures 13 and 14 are results from an experimental run that encountered problems by the detector, which occurred for no apparent reason during this specific sample run. Consequently, this occurrence resulted in lost signal counts below the zero line which does not give a clear measurement for total areas created under the curves. Even through the detector arbitrary went to zero, this data set still serves useful in giving clear indications of curve peaks, which show that curve peak height is dependent on Cl<sup>-</sup> interference.

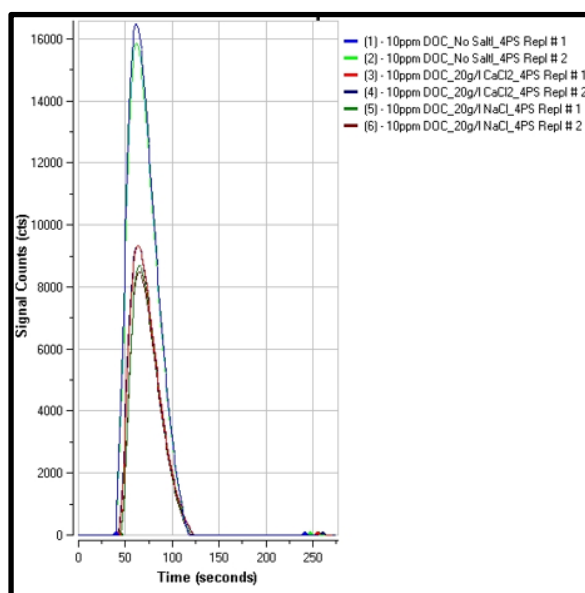


Figure 13. Chloride interference data for 10ppm DOC concentrations retrieved from OI Analytical Aurora (TICTOC) reports.

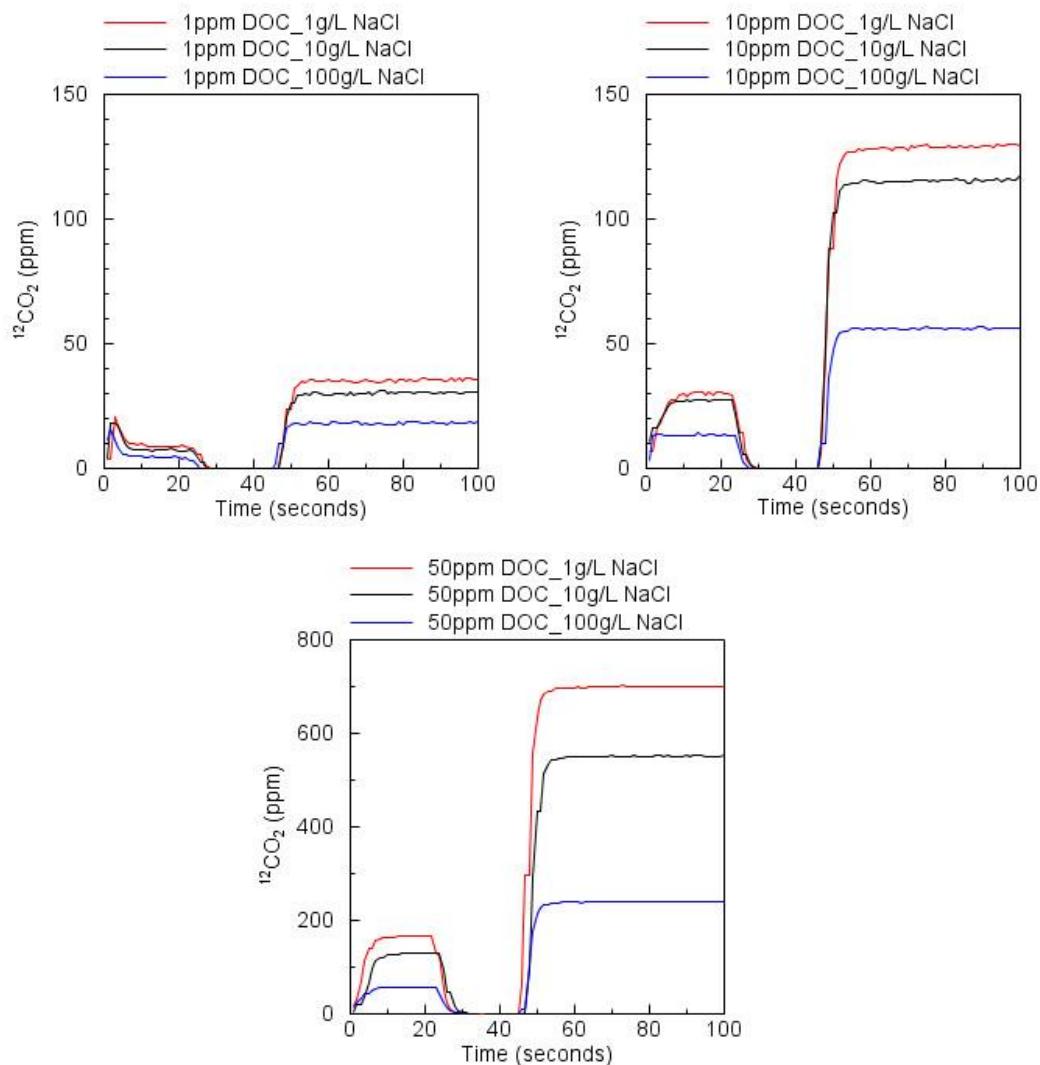


Figure 14. Data results of chloride effect in DOC concentrations retrieved and created using CRDS reports.

In order to analyze complex brines that may contain different salt compounds, potential chloride interference was investigated using DOC solutions containing variable concentrations of NaCl or CaCl<sub>2</sub>. Measurements show very little difference in CO<sub>2</sub> recovery when comparing solutions with equal chloride content from NaCl versus CaCl<sub>2</sub>. However, solid precipitate, presumably gypsum (CaSO<sub>4</sub>), formed in the reaction chamber in increasing amounts with higher CaCl<sub>2</sub> concentrations. Increasing the volume of sodium persulfate reagent during the oxidation of DOC solutions containing high levels of calcium must be approached with caution, due to the potential precipitation of CaSO<sub>4</sub> in the reaction chamber which may plug tubing. Therefore to avoid precipitation of CaSO<sub>4</sub>, experiments were conducted at maximum 20 g/L Cl<sup>-</sup> as CaCl<sub>2</sub>. Results show little variability in DOC oxidation and CO<sub>2</sub> recovery in the presence of either NaCl or CaCl<sub>2</sub> (Figure 15).

Method developments also sought to optimize DOC oxidation by increasing the amount of sodium persulfate reagent in an effort to overwhelm the inhibiting effect of chloride and the natural decomposition of sodium persulfate. Measurements show that by increasing volume of sodium persulfate reagent from 2 ml to 4 ml increased DOC oxidation and improved total CO<sub>2</sub> recovery by approximately 6-8% in experimental solutions containing 10ppm C as KHP and 10 g/L NaCl chloride solutions and approximately 10% in 10ppm acetic acid containing 10 g/L NaCl and CaCl<sub>2</sub> chloride solutions (Figure 16). Results show that DOC solutions with salinity as low as 1 g/L NaCl display similar CO<sub>2</sub> recovery when reacted with 2 ml or 4 ml of the oxidizing reagent. Results for 1ppm DOC 10g/L NaCl solution show that recovered CO<sub>2</sub> increased about 20ppm when reacted to 4 ml sodium persulfate versus 2 ml of sodium persulfate (Figure 17).

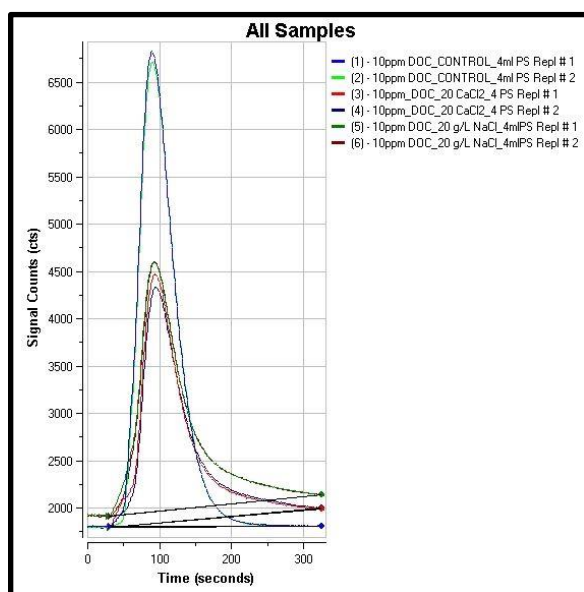


Figure 15. NaCl (dark green and dark red curves) versus  $\text{CaCl}_2$  (red and black curves) concentrations in 10 ppm DOC experimental solutions retrieved from OI Analytical Aurora (TICTOC) reports.

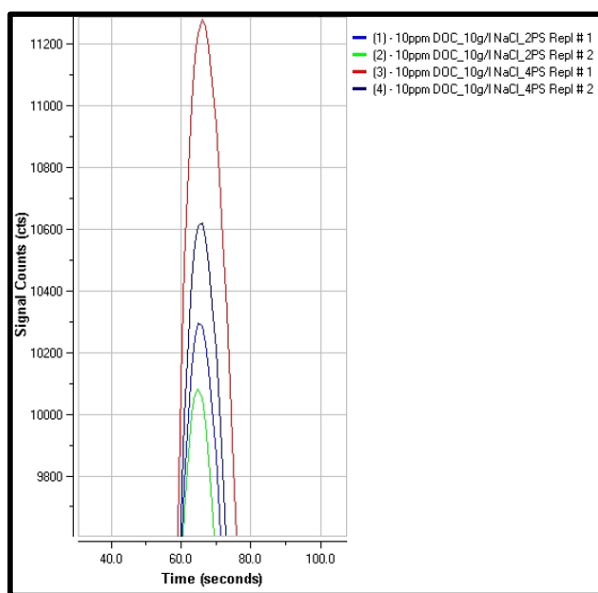


Figure 16. 2 ml (bottom two curves: blue and green) vs. 4 ml (top two curves: red and black) volume of oxidizing reagent data for 10 ppm DOC containing 10g/L NaCl concentrations retrieved from OI Analytical Aurora (TICTOC) reports.



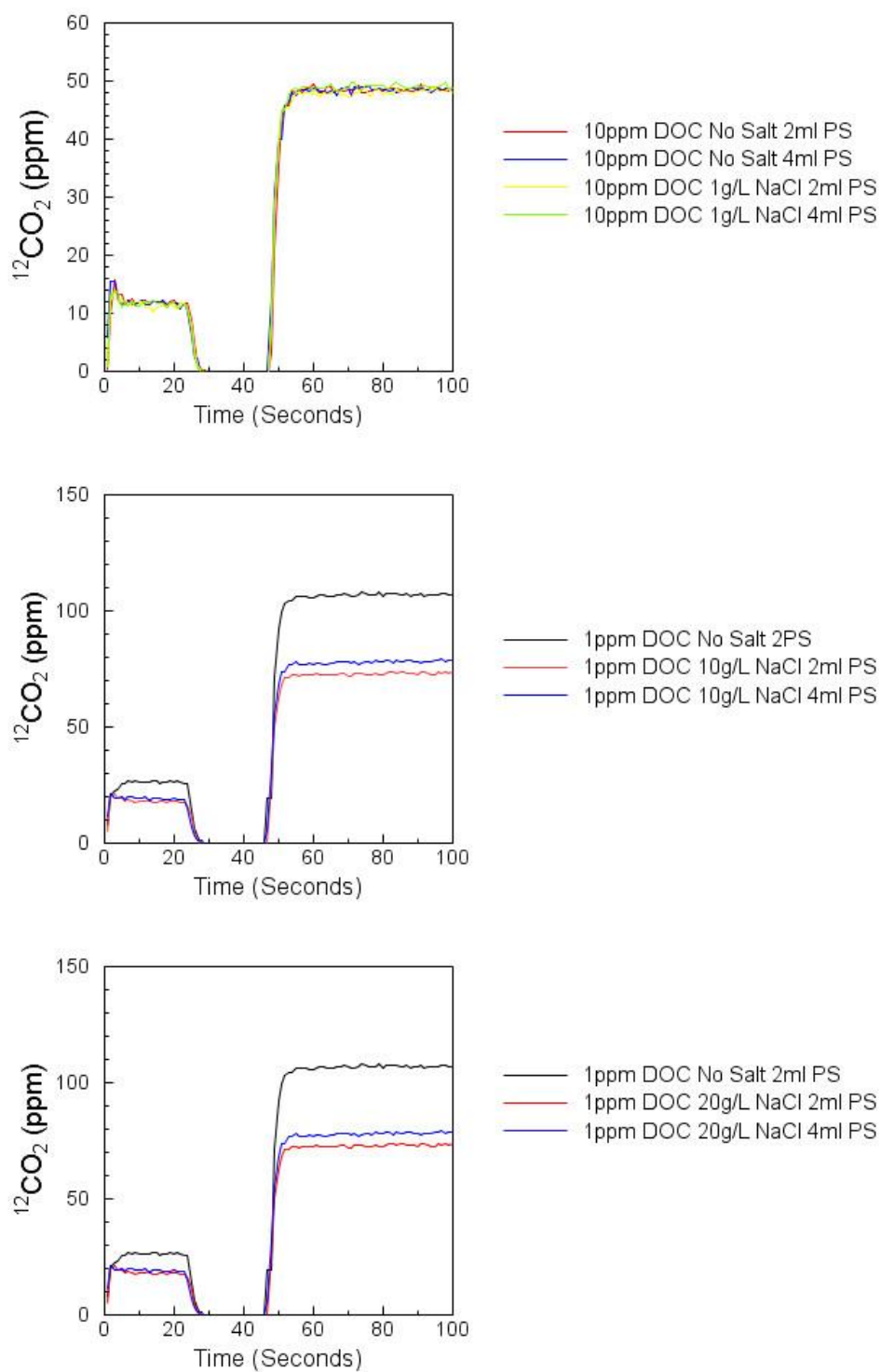


Figure 17. 2 ml vs. 4 ml volume of oxidizing reagent data for DOC no salt solutions and DOC salt solutions retrieved and created using CRDS reports.

#### 4.2.2 Picarro CRDS

Results from analysis of 1ppm C as DOC at various NaCl concentrations give immense variability for  $\delta^{13}\text{C}$  signals. However, as DOC concentrations increased with NaCl concentrations, the  $\delta^{13}\text{C}$  signals became less variable and more reliable. As seen in results from 50ppm DOC solutions containing 1 g/L, 10 g/L, or 100 g/L NaCl concentrations,  $\delta^{13}\text{C}$  signals displayed less variability (Figure 18).

$\delta^{13}\text{C}$  concentration measurements of KHP and acetic acid, as a function of chloride concentration, calculated from CRDS data logs are shown below (Figures 19A and 19B). Results show  $\delta^{13}\text{C}$  signals significantly change with increasing chloride concentrations, presumably due to incomplete oxidation. Results of  $\delta^{13}\text{C}$  measurements of KHP solutions with elevated salinity show small variability in the  $\delta^{13}\text{C}$  despite the incomplete oxidation as chloride interference increases (Figure 19A). However, results show oxidation of KHP was very different than for acetic acid. These results were unexpected due to initial assumptions that considered the simpler molecular structure of acetic acid less problematic. Although oxidation of 10ppm acetic acid produced approximately 14% more  $\text{CO}_2$  concentration, the  $\delta^{13}\text{C}$  concentration measurements show large systematic decrease in apparent isotope composition with increased salt content and inhibited oxidation (Figure 19B).

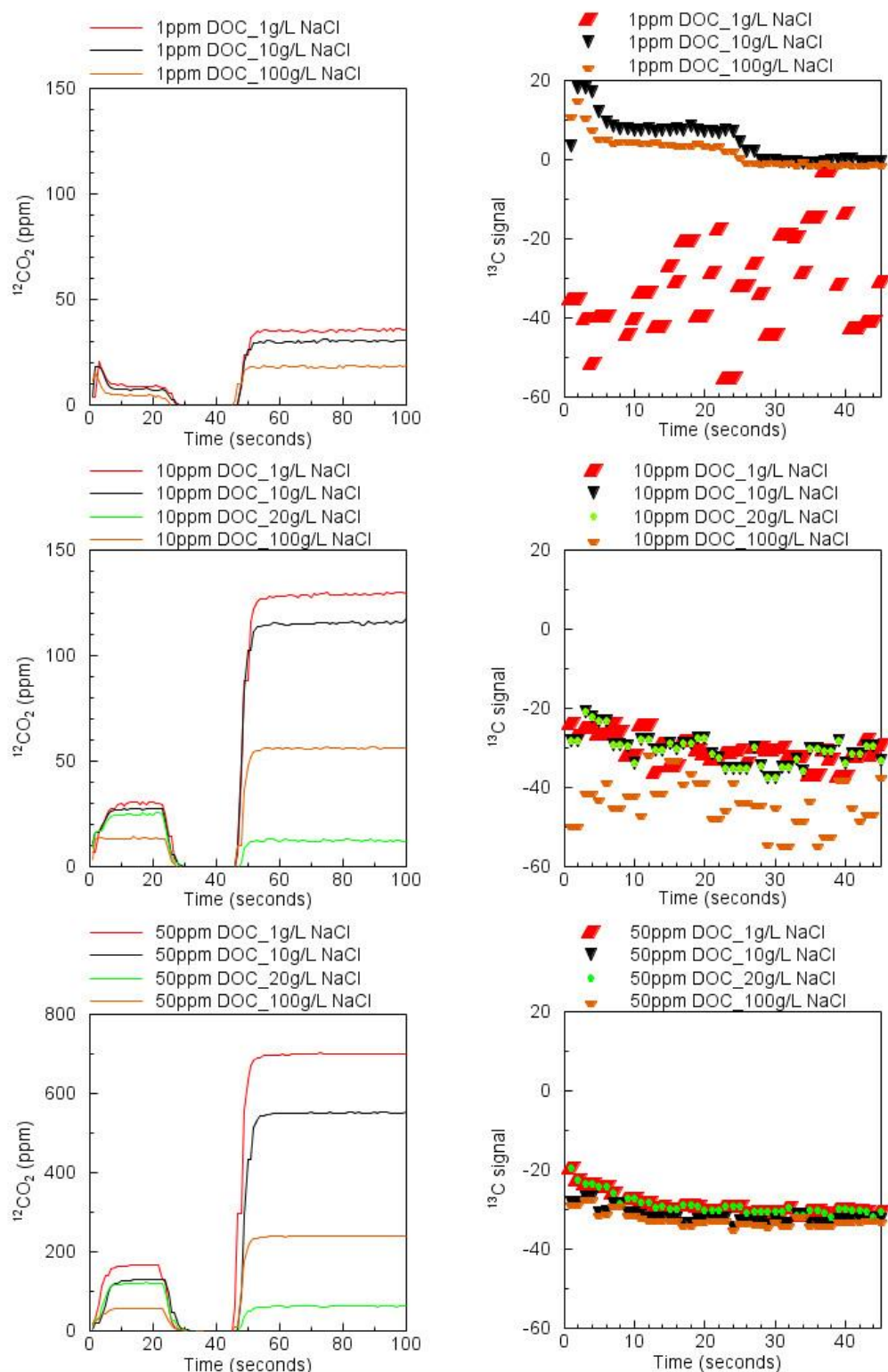
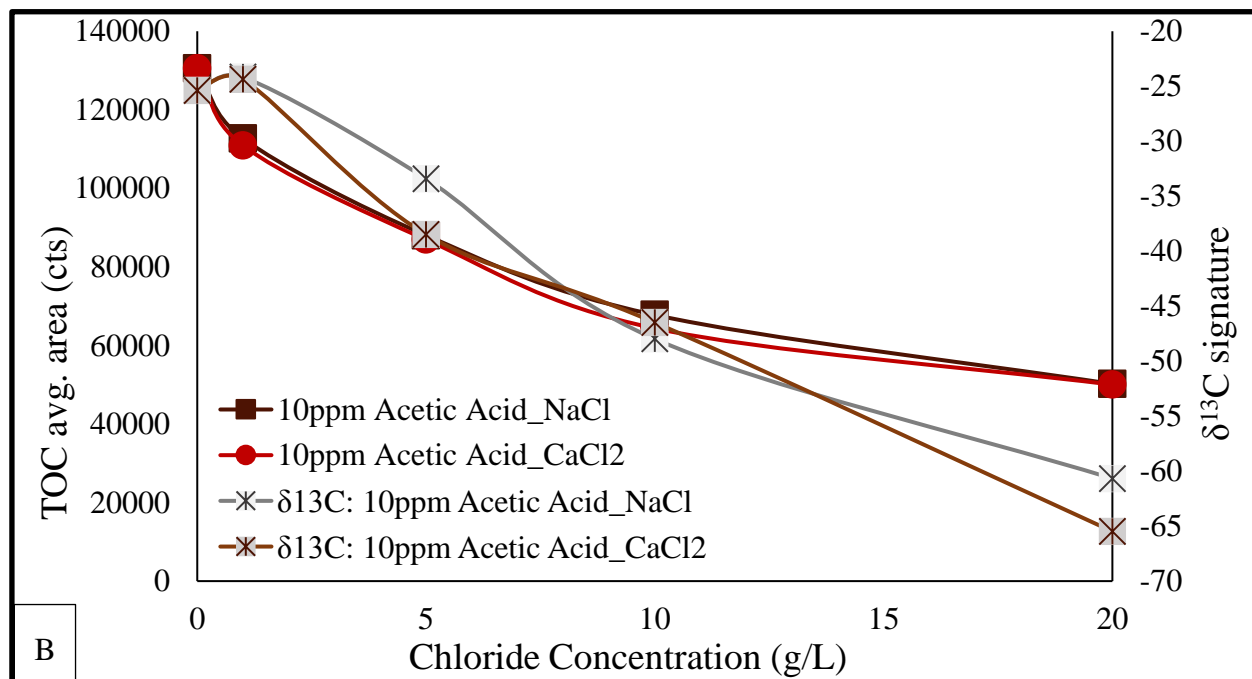
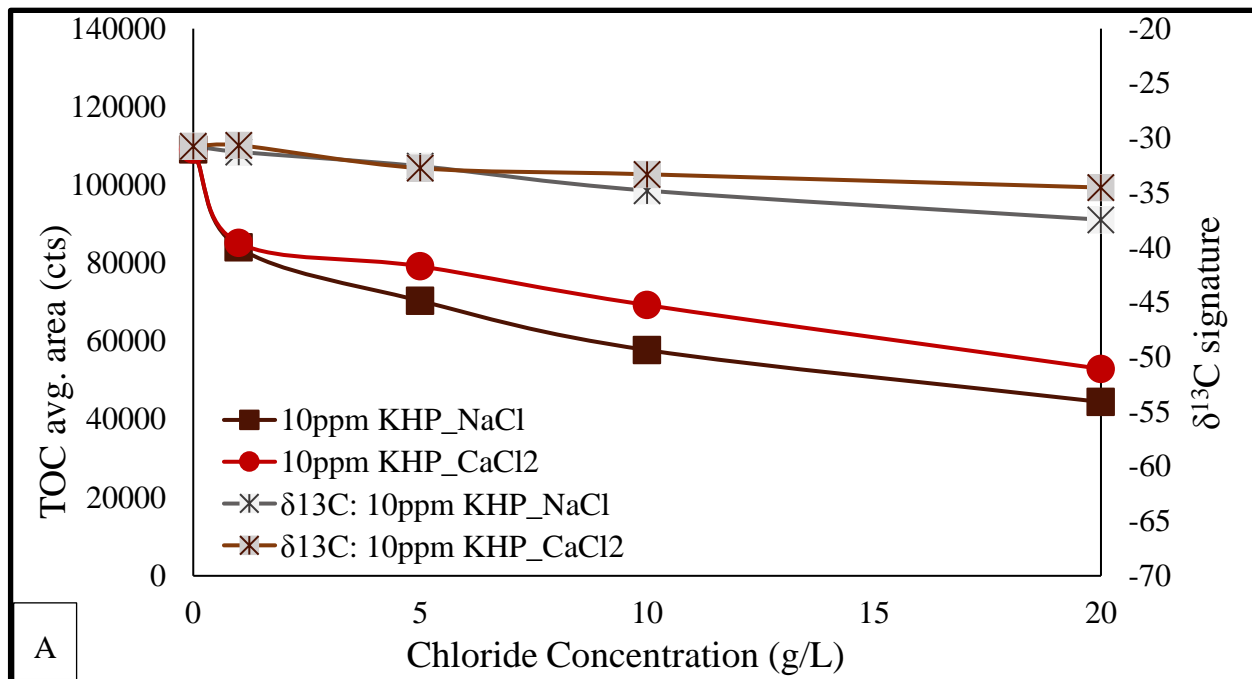


Figure 18. Recovered  $\text{CO}_2$  concentration and measured  $\delta^{13}\text{C}$  signals data results for DOC experimental solutions covering a range of concentration and salinity. It is important to note that  $\text{CO}_2$  concentrations measured for both 10ppm and 50ppm DOC with 20 g/L NaCl (green curves) are lower than expected, but the measured  $\delta^{13}\text{C}$  signals appear to show similar trends compared to all other solutions. Retrieved and created using TICTOC and CRDS reports.



Figures 19. Maximizing CO<sub>2</sub> recovery data, for A) KHP and B) acetic acid concentrations, retrieved from TICTOC reports and δ<sup>13</sup>C concentration measurements retrieved from CRDS data logs.

### 4.3 Field Samples

Total DIC concentrations for freshwater input samples show low DIC concentrations compared to higher DIC concentration measurements in flowback samples. The large variability in U/PtP-C-flbck on day 5 through day 15 may have been caused by drill pipe hardware changes during well production procedures (Figure 20). Flowback fluids have as much as a four-fold increase in DIC concentration than input fluids (Figure 21).

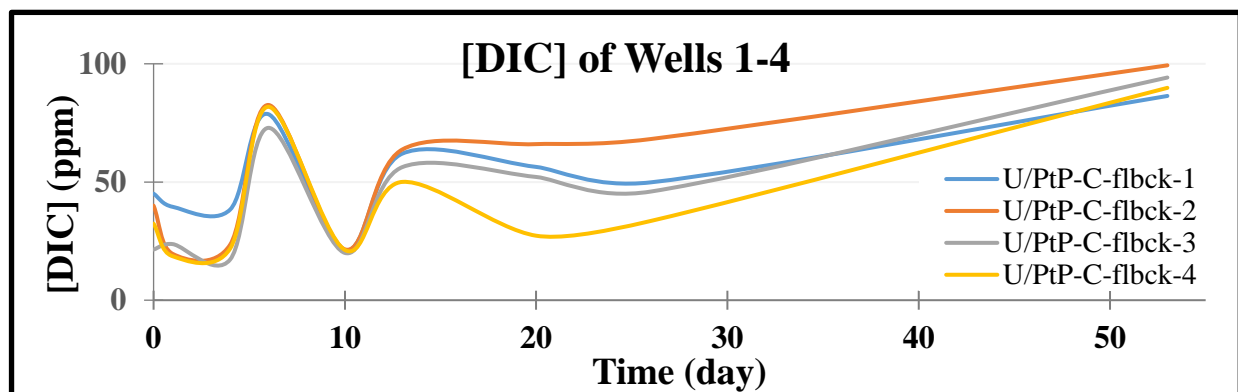


Figure 20. DIC concentration results for field samples. Data was measured by the TICTOC data reports.

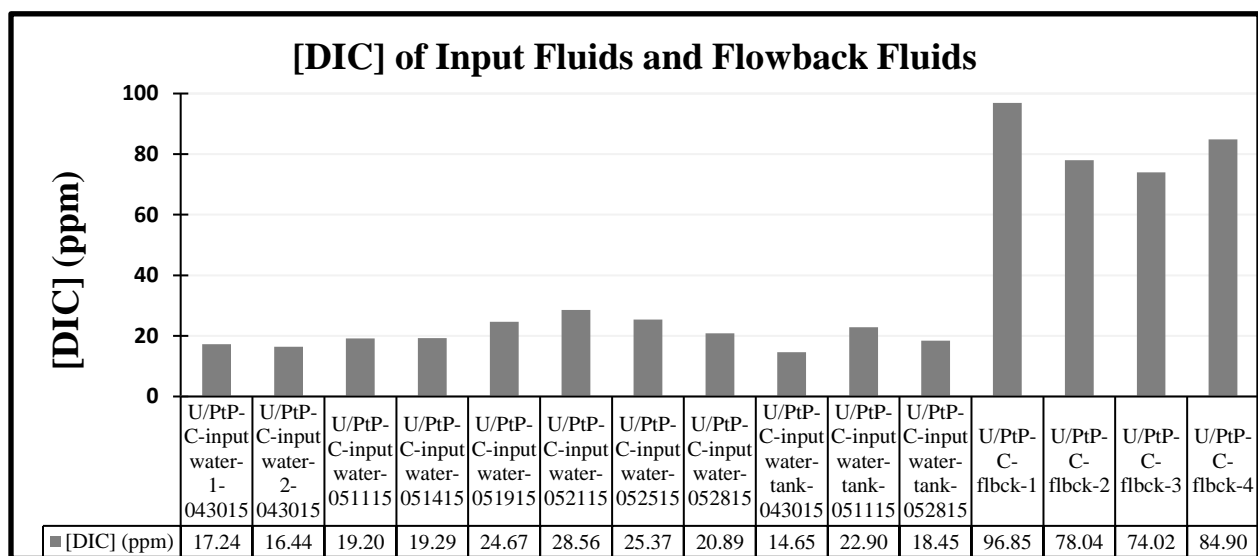


Figure 21. DIC concentration results for field samples. Data was measured by the TICTOC data reports.

$\delta^{13}\text{C}$  of DIC in flowback fluids varies greatly among the four wells and over time (Figure 22). The large variability in U/PtP-C-flbck on day 5 through day 15 may have been caused by drill pipe hardware changes during well production procedures.  $\delta^{13}\text{C}$  measurements for freshwater input samples and hydraulic fracturing flowback samples show that flowback fluids are significantly isotopically heavier than input fluids (Figure 23).

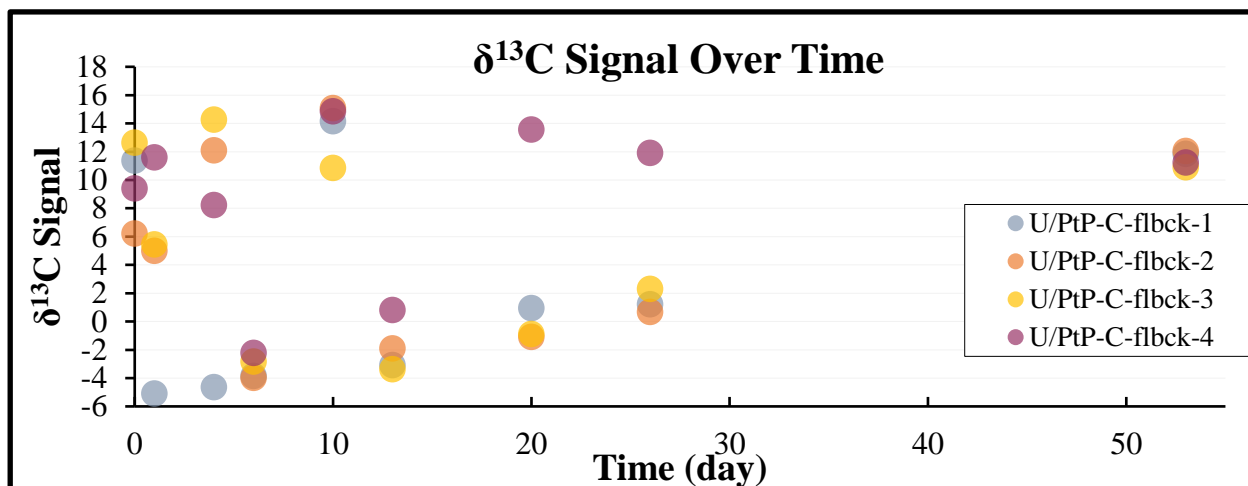


Figure 22.  $\delta^{13}\text{C}$  data for DIC results for field samples obtained from the CRDS data logs.

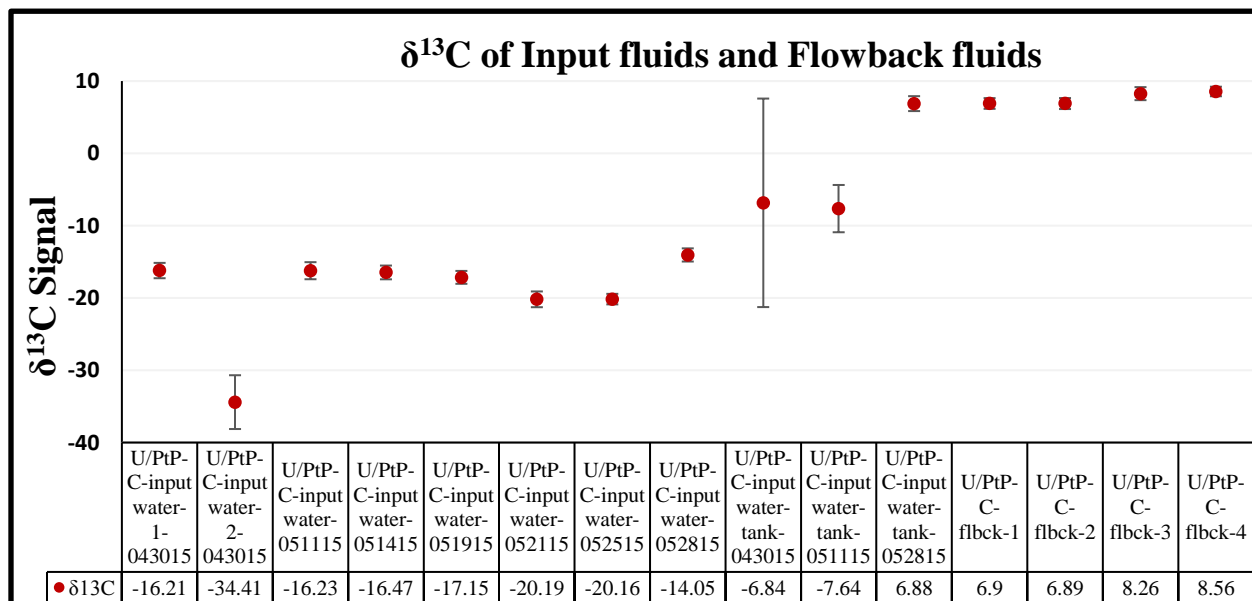


Figure 23.  $\delta^{13}\text{C}$  data for DIC results for field samples obtained from the CRDS data logs.

Due to inadequate recovered  $\text{CO}_2$  concentrations from WCO of DOC in flowback fluids,  $\delta^{13}\text{C}$  signals data results exhibit significant variability and are unreliable (Figure 24).

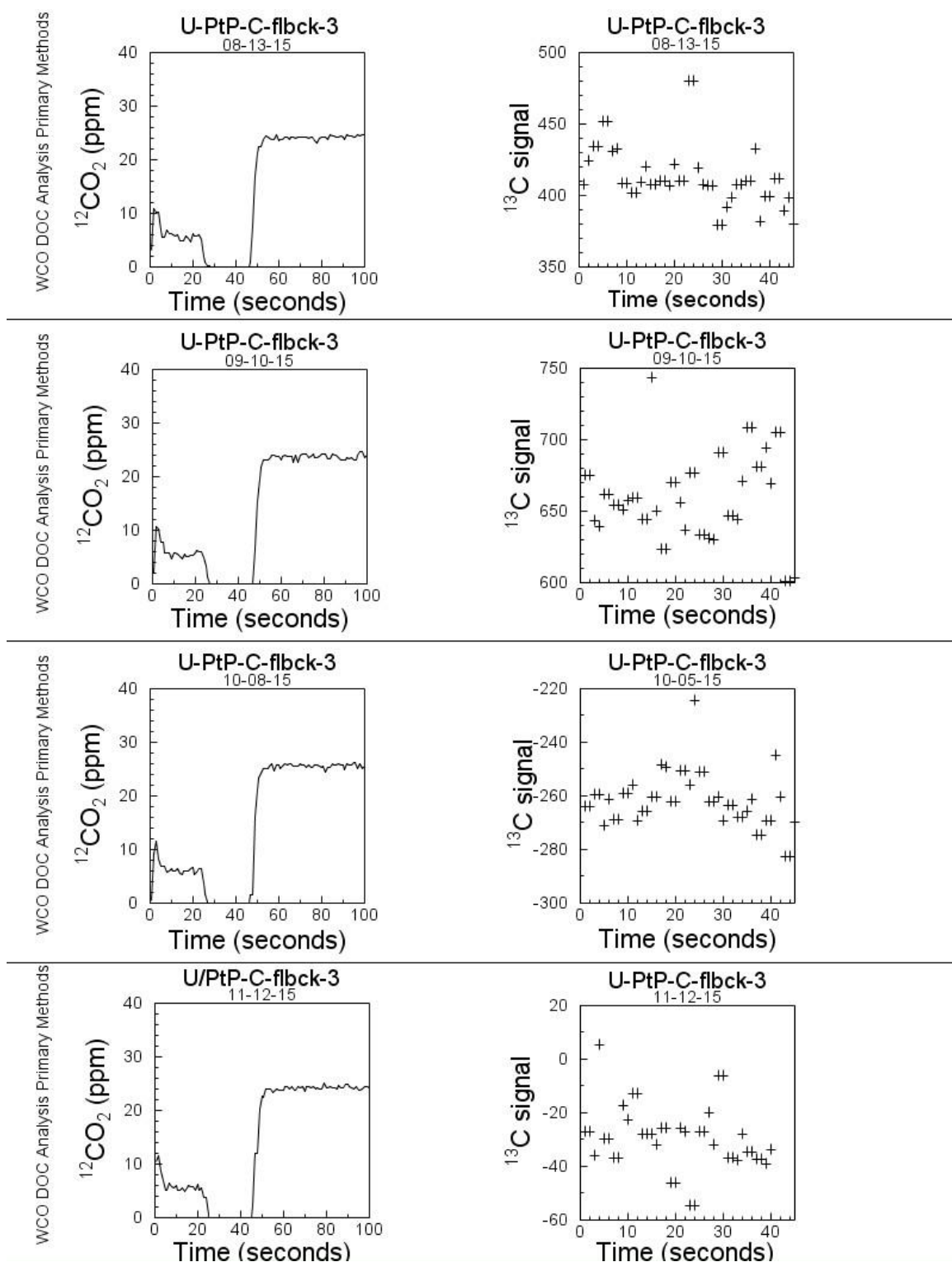


Figure 24.  $\delta^{13}\text{C}$  data for DOC concentrations for field samples retrieved from CRDS data logs.

## DISCUSSION

DIC methods for extending reaction and detection times is an effective technique for DIC analysis of solutions with salinities as high as 200 g/L NaCl. With extending reaction and detection times, the instruments ability to recover CO<sub>2</sub> was improved. In addition, the recovery of CO<sub>2</sub> concentrations from DIC solutions were unaffected by chloride, even at the high concentrations expected for flowback fluids.

The  $\delta^{13}\text{C}$  signals for DIC solutions varied with CO<sub>2</sub> concentrations however measurements show at lower DIC concentrations,  $\delta^{13}\text{C}$  signals appear variable and are unreliable. Whereas DIC concentrations of 20ppm and higher give  $\delta^{13}\text{C}$  that show less variability than 10ppm DOC solutions. DIC analysis of experimental solutions that covered a range of DIC and salinity concentrations expected for flowback fluids, show relatively stable  $\delta^{13}\text{C}$  signals when recovered CO<sub>2</sub> concentrations are high and little fractionation in the  $\delta^{13}\text{C}$  compositions.

Similar to DIC methods, extending WCO of DOC reaction and detection times is an effective technique for DOC analysis. Methods implemented to oxidize DOC and recover CO<sub>2</sub> in low salt solutions by using the WCO technique show total CO<sub>2</sub> recovery is dependent on concentrations of organic matter in solution. DOC salt free experimental solutions exhibit more complete oxidation of DOC to CO<sub>2</sub> and it is determined that CO<sub>2</sub> recovery increases as the function of DOC concentration increases.

Similar to what was observed for the DIC solutions, the  $\delta^{13}\text{C}$  signals from the CRDS for all DOC solutions analyzed vary as a function of CO<sub>2</sub> concentrations. Measurements clearly show that  $\delta^{13}\text{C}$  signal in the CRDS are more stable and reproducible at high DOC concentrations. At lower DOC concentrations, which are typically found in freshwater/natural samples, there is

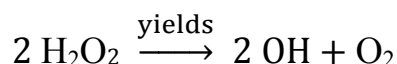
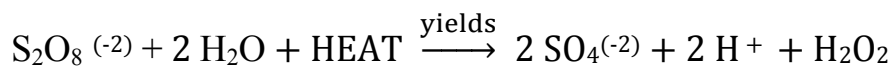
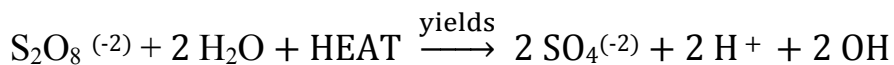
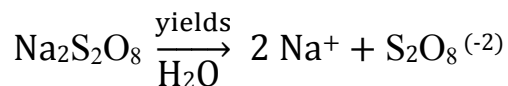


considerable variability in CRDS  $\delta^{13}\text{C}$  signal, hence analysis for low DOC concentrations may be difficult (Hartland et al., 2012).

Measurements of DOC solutions with elevated salinity clearly show limited recovery of  $\text{CO}_2$ . The incomplete oxidation of organic matter in saline solutions is due to chloride interference which inhibits  $\text{CO}_2$  recovery. These results are similar to those described by McKenna and Doering (1995), and Conaway et al. (2015). The inhibition of DOC oxidation is attributed to the competition between DOC and chloride ions available to react with sodium persulfate reagent (Barber, 2015). The reaction rate for chloride is estimated at  $2 \times 10^8 \text{ (mgL)}^{-1} \text{ s}^{-1}$  to  $3.5 \times 10^9 \text{ (mgL)}^{-1} \text{ s}^{-1}$ , respectively (Osburn and St-Jean, 2007) compared to the reaction rate for organics estimated at  $1 \times 10^4 \text{ (mgL)}^{-1} \text{ s}^{-1}$  with an upper bound of  $2 \times 10^4 \text{ (mgL)}^{-1} \text{ s}^{-1}$  (Peyton, 1993) and the hypothesis suggests with increased salinity, chloride ions quickly and readily consume sodium persulfate which in turn decreases the sodium persulfate reagent's potential to oxidize DOC. DOC analysis of solutions with elevated salinity exhibit a considerable error in the CRDS  $\delta^{13}\text{C}$  signals. Similarly, Osburn and St-Jean (2007) also reported dramatic changes in  $\delta^{13}\text{C}$  signatures when analyzing DOC samples in chloride-containing solutions, which they suggested was due to the incomplete oxidation of DOC due to the chloride interference.

By increasing the volume of sodium persulfate reagent to maximize DOC oxidation, our results show that the technique is only effective in high salinity solutions (Figure 17). DOC solutions containing low chloride concentrations ( $<1\text{g/L Cl}^-$ ) show no variability in  $\text{CO}_2$  recovery, thus determining that increasing oxidizing reagent volume is unnecessary due to decreased chloride inhibition. Although, as chloride concentrations increase ( $\geq 10\text{g/L Cl}^-$ ), increasing oxidizing reagent volume is effective for attaining increased  $\text{CO}_2$  resulting from WCO

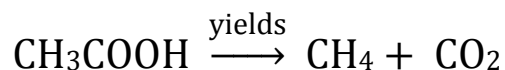
of DOC. The following chemical reactions describe how sulfate and hydroxyl radicals form during sodium persulfate chemical reactions:



Our WCO conditions for the oxidizing reagents method differ from those of a previous study conducted by Hartland et al. (2012), who reports successful use of the TICTOC when analyzing low salinity samples with a DOC concentration < 2.5 mg/L. Their study achieved maximum oxidation at low (2.5 mg/L) DOC concentration by adjusting the addition equivalent to 0.4 ml of 25% phosphoric acid (~ 0.1 ml phosphoric acid) and 0.7 ml of 30% sodium persulfate (~ 0.21 ml sodium persulfate) to 9 ml of sample solutions. Our study adjusted the addition of 1.0 ml of 5% phosphoric acid (~0.05 ml phosphoric acid) and 2 ml or 4 ml of 10% sodium persulfate (~0.2 ml or 0.4 ml sodium persulfate) to 5 ml of sample solution. In comparison to Hartland et al.'s study, our experiments used half of the phosphoric acid reagent to purge DIC and utilized almost twice as much sodium persulfate reagent to oxidize DOC. Sodium persulfate activation pathways form sulfate and hydroxyl radicals which are very strong oxidants for any species susceptible to oxidation, such as organic material and halides (Osburn and St-Jean, 2017). According to Osburn and St-Jean (2007), these oxidation susceptible species readily compete to react with sulfate radicals, thereby consuming sulfate radicals quickly. Hydraulic fracturing fluids frequently have high salinity, in excess of 100 g/L  $\text{Cl}^-$ , which reduces

the potential for sulfate radicals to react with organic carbon compounds because of chloride interference.

Hydraulic fracturing fluids are complex solutions containing numerous organic compounds, thus prompting further investigation of optimizing DOC oxidation relative to different organic compounds. Maximizing CO<sub>2</sub> recovery not only shows a dependence on the concentrations of DOC, but also could very well be influenced by the quality and quantity of organics susceptible to oxidation. McKenna and Doering (1995) identified possible differences in the nature and quantity of organic matter during oxidation, but affirmed the degree of interference from chloride is more substantial. Most experimental solutions tested in this study used KHP as a typical organic compound. However, flowback fluid contains a myriad of organic compounds, and of these, acetate was one of the most abundant organic compounds detected by ion chromatography in the flowback fluid. Therefore, acetic acid was selected for additional experiments. Acetate is a simple organic molecule which was expected to oxidize more rapidly and completely. Analysis of 10ppm DOC solutions show that the oxidation of acetic acid recovered more CO<sub>2</sub> than KHP at salinity concentrations < 20g/L, suggesting that acetic acid experienced more complete oxidation. In contrast, when 10ppm DOC concentrations contained >10 g/L salinity, results show little variability in the recovered CO<sub>2</sub>. The reaction pathway for oxidation of acetic acid with sodium persulfate decomposes acetic acid into methane and carbon dioxide. Nimmanwudipong et al. (2015) demonstrated that CO<sub>2</sub> evolved by this catalytic reaction is produced solely from the carboxyl compound (COOH<sup>-</sup>) of the acetic acid and infers the following chemical reaction,



Measurements show dissimilarity of  $\delta^{13}\text{C}$  signals of 10ppm KHP compared to 10ppm acetic acid. The large variability in  $\delta^{13}\text{C}$  signals for acetic acid solutions over a range of salt concentrations may be due to kinetic isotope fractionation processes. As discussed by Clark and Fritz (1997), like elements within the same compound may demonstrate differences of bond strengths for isotopes which provide differences in reaction rates. This suggests that kinetic isotope fractionation of acetic acid involves variations in the reaction rates for different  $\delta^{13}\text{C}$  concentrations of the carboxyl group versus the methyl group ( $\text{CH}_3$ ). Our results may indicate lighter  $\delta^{13}\text{C}$  concentrations within the  $\text{CO}_2$  is produced solely from the carboxyl compound ( $\text{COOH}^-$ ). Light isotope bonds, evident in ( $\text{COOH}^-$ ), build weaker bonds therefore reacting more quickly to oxidizing conditions (Clark and Fritz, 1997). Therefore, it is concluded that this study measured  $\delta^{13}\text{C}$  measurements representing  $\delta^{13}\text{C}_{(\text{COOH}^-)} = \delta^{13}\text{C}_{(\text{CO}_2)}$  concentrations.

## CONCLUSIONS

The research herein has documented method developments to improve analysis of carbon species in solutions containing elevated salinity, such as flowback fluids, using a carbon analyzer interfaced with a CRDS. These method developments explored DIC acidification and DOC oxidation in order to enhance CO<sub>2</sub> evolution for subsequent  $\delta^{13}\text{C}$  measurements. DIC method developments focused on extending both reaction and detection times of the instrument and demonstrated to be an effective technique for recovering increased CO<sub>2</sub> concentrations. DIC method developments showed that elevated chloride does not affect CO<sub>2</sub> evolution. Analysis of the isotopic composition of the DIC solutions showed that for concentrations as low as 1ppm C as DIC produce reliable  $\delta^{13}\text{C}$  measurements. Variability of  $\delta^{13}\text{C}$  measurements are dependent on CO<sub>2</sub> concentrations analyzed by the CRDS, thus emphasizing that maximum CO<sub>2</sub> recovery is essential for accurate analysis.

DOC method development posed challenges. WCO techniques for DOC solutions with elevated salinity must overcome many factors, especially high chloride interference. This study concluded that WCO and CO<sub>2</sub> recovery can be improved by extending both reaction and detection times during the oxidation step. DOC method developments also confirmed that increasing the volume of oxidizing reagent volume increased DOC oxidation thereby improving CO<sub>2</sub> recovery. Since produced fluids contain different salt compounds, this research investigated potential effects of both NaCl and CaCl<sub>2</sub> on WOC reactions and concluded that CO<sub>2</sub> recovery is similar for solutions with equal chloride content, hence indicating that Cl<sup>-</sup> interference is the limiting factor. Overall, DOC analysis demonstrated that salinity as low as 10g/L in a 1ppm DOC solution resulted in incomplete oxidation thus hindering CO<sub>2</sub> recovery. DOC method development further showed that DOC compounds oxidize differently resulting in large systematic variation in  $\delta^{13}\text{C}$  measurements. DOC methods were unsuccessful in attaining reliable

and reproducible  $\delta^{13}$  measurements for solutions of high salinity and low DOC concentrations because of limited  $\text{CO}_2$  recovery. Nevertheless, extending reaction and detection times along with increasing oxidizing reagent are approaches that can be applied in future WCO techniques. Since DOC  $\delta^{13}\text{C}$  measurements are dependent on  $\text{CO}_2$  concentrations evolved from WCO, we emphasize that improving  $\text{CO}_2$  recovery through overcoming chloride interference is essential for further analysis.

## **RECOMMENDATIONS FOR FUTURE WORK**

Future method developments to optimize CO<sub>2</sub> recovery using wet chemical oxidation techniques for samples containing DOC with high salinity is recommended. Future method developments should focus on overcoming chloride interface that occurs during wet chemical oxidation reactions. This research used sodium persulfate as an oxidizing reagent. Possible future method developments could investigate use of different oxidizing reagents. Future research should also investigate use of high temperature combustion (HTC) techniques for analyzing high salinity solutions such as produced fluids.

## REFERENCES CITED

- Barber, A., Lalonde, K., Gélinas, Y. (2015). Measuring the  $\delta^{13}\text{C}$  Signature of Dissolved Organic Carbon: An Inter-laboratory Comparison Study [Poster]. Retrieved on January 23, 2017. <http://stableisotopefacility.ucdavis.edu/ASITA/Barber-poster.pdf>.
- Clark, I., and Fritz, P. (1997). Environmental Isotopes in Hydrology. Boca Raton, Florida: Lewis Publishers.
- Conaway, C. H., Thomas, B., Saad, N., Thordsen, J. J., & Kharaka, Y. K. (2015). Carbon isotope analysis of dissolved organic carbon in fresh and saline (NaCl) water via continuous flow cavity ring-down spectroscopy following wet chemical oxidation. *Isotopes in Environmental and Health Studies*, 51, 2, 344-358. <http://dx.doi.org/10.1080/10256016.2015.1009910>.
- Harrington, J., Cole, D., Sheets, J., Swift, A., Murphy, M., Welch, S. (2013). TOC and Mineralogical Trends in the Utica Shale of Ohio. [Abstract]. AAPG 2013 Annual Convention and Exhibition, Article #90163. Retrieved on February 14, 2017. <http://www.searchanddiscovery.com/abstracts/html/2013/90163ace/abstracts/harr.htm>.
- Hartland, A., Baker, A., Timms, W., Shutova, Y., & Yu, D. (2012). Measuring dissolved organic carbon  $\delta\text{C}$  in freshwaters using total organic carbon cavity ring-down spectroscopy (TOC-CRDS). *Environmental Chemistry Letters*, 10(3), 309-315. doi:10.1007/s10311-012-0377-z.
- Hickman, J., Eble, C., and Harris, D. (2015a). Lithostratigraphy, in Patchen, D.G. and Carter, K.M., eds., A geologic play book for Utica Shale Appalachian basin exploration, Final report of the Utica Shale Appalachian basin exploration consortium, p. 19-21, Retrieved on February 11, 2017. <http://www.wvgs.wvnet.edu/utica>.
- Hickman, J., Eble, C., and Harris, D. (2015b). Lithostratigraphy, in Patchen, D.G. and Carter, K.M., eds., A geologic play book for Utica Shale Appalachian basin exploration, Final report of the Utica Shale Appalachian basin exploration consortium, Appendix 3-A, Utica and equivalent outcrop descriptions by state. Retrieved on February 11, 2017. [http://www.wvgs.wvnet.edu/utica/playbook/docs/AP\\_3A\\_FINAL.pdf](http://www.wvgs.wvnet.edu/utica/playbook/docs/AP_3A_FINAL.pdf).
- Kendall, C., and McDonnell, J. J. (1999). Isotope Tracers in Catchment Hydrology. *Hydrological Sciences Journal = Journal Des Sciences Hydrologiques*, 44, 6, 998. Retrieved on April 1, 2017. <http://www.rcamnl.wr.usgs.gov/isoig/isopubs/itchch2.html>.
- King, G. E. (2012). Hydraulic Fracturing 101: What Every Representative, Environmentalist, Regulator, Reporter, Investor, University Researcher, Neighbor, and Engineer Should Know About Hydraulic Fracturing Risk. Society of Petroleum Engineers. doi:10.2118/0412-0034-JPT.
- Kondash, A. J., Albright, E., and Vengosh, A. (2017). Quantity of flowback and produced waters from unconventional oil and gas exploration. *Science of the Total Environment*, 574, 314-321. <http://doi.org/10.1016/j.scitotenv.2016.09.069>.
- McClain, T. (2012). Sequence Stratigraphy Interpretation of the Utica Shale and Associated Late Ordovician Strata, Eastern Ohio and Western Pennsylvania. [Abstract]. AAPG Search and Discovery Article #90152. Retrieved on February 11, 2017. <http://www.searchanddiscovery.com/abstracts/html/2012/90152sw/abstracts/mccl.htm>.



- McKenna, J. H., and Doering, P. H. (1995). Measurement of dissolved organic carbon by wet chemical oxidation with persulfate: influence of chloride concentration and reagent volume. *Marine Chemistry*, 48, 2, 109-114. [http://dx.doi.org/10.1016/0304-4203\(94\)00049-J](http://dx.doi.org/10.1016/0304-4203(94)00049-J).
- Nimmanwudipong, T., Yoshida, N., Gilbert, A., Yoshida, N., Yamada, K., & Yoshida, N. (2015). Analytical method for simultaneous determination of bulk and intramolecular <sup>13</sup>C-isotope compositions of acetic acid. *Rapid Communications in Mass Spectrometry*, 29(24), 2337-2340. doi:10.1002/RCM.7398.
- Osburn, C., and St-Jean, G. (2007). The use of wet chemical oxidation with high-amplification isotope ratio mass spectrometry (WCO-IRMS) to measure stable isotope values of dissolved organic carbon in seawater. *Limnology and Oceanography: Methods*, 5:296-308. doi:10.4319/lom.2007.5.296.
- Peyton, G. R. (1993). The free-radical chemistry of persulfate based total organic carbon analyzers. *Mar. Chem.* 41:91103. [https://doi.org/10.1016/0304-4203\(93\)90108-Z](https://doi.org/10.1016/0304-4203(93)90108-Z).
- Picarro. Cavity Ring-Down Spectroscopy (CRDS). (2017). Retrived on March 21, 2017. [http://www.picarro.com/technology/cavity\\_ring\\_down](http://www.picarro.com/technology/cavity_ring_down).
- Smith, L. B. (2014). Sedimentology, Stratigraphy, Organic Content, and Reservoir Characteristics of Utica Shale Cores, Central Ohio [Abstract]. AAPG Datapages/Search and Discovery Article #90195. Retrieved on February 11, 2017. <http://www.searchanddiscovery.com/abstracts/html/2014/90195eastern/abstracts/35>.
- The Ohio Department of Natural Resources. (2017). Ohio Oil and Gas Well Database. Retrieved on January 31, 2017. <https://apps.ohiodnr.gov/oilgas/rbdrsreports/>.
- The Ohio Department of Natural Resources. Maximum TOC Value per Well of the Upper Ordovician Shale Interval of Ohio. (2013). Retrieved on February 11, 2017. [http://geosurvey.ohiodnr.gov/portals/geosurvey/Energy/Utica/Ordov-Shale\\_TOC-Max\\_03-2013.pdf](http://geosurvey.ohiodnr.gov/portals/geosurvey/Energy/Utica/Ordov-Shale_TOC-Max_03-2013.pdf).
- Vazquez, O., Mehta, R., Mackay, E., Linares-Samaniego, S., Jordan, M., and Fidoie, J. (2014). Post-frac Flowback Water Chemistry Matching in a Shale Development. Society of Petroleum Engineers. <https://doi.org/10.2118/169799-MS>.
- Wangersky, P. J. (1993). Dissolved organic carbon methods: a critical review. *Marine Chemistry*, 41, 1, 61-74. [http://dx.doi.org/10.1016/0304-4203\(93\)90106-X](http://dx.doi.org/10.1016/0304-4203(93)90106-X).
- Wattenbarger, R. A., and Alkough, A. B. (2013). New Advances in Shale Reservoir Analysis Using Flowback Data. Society of Petroleum Engineers. <https://doi.org/10.2118/165721-MS>.

## APPENDICES

Table 1. UtPtP-C-2-flbk\_714 flowback fluid raw data for DIC analysis where “sniff” and “pulse” peaks are indentified.

	UtPtP-C-2-flbk_714		
DATE	12CO2	13CO2_Raw	Delta_Raw
9/10/2015	0.57	0.10	3778.30
9/10/2015	0.57	0.10	3778.30
9/10/2015	27.91	0.29	-488.82
9/10/2015	46.69	0.29	-488.82
9/10/2015	98.06	0.86	-249.95
9/10/2015	151.47	1.52	-132.53
9/10/2015	180.53	1.94	-67.57
9/10/2015	180.53	1.94	-67.66
9/10/2015	198.20	2.28	-18.24
9/10/2015	202.52	2.28	-18.24
9/10/2015	205.49	2.33	-14.10
9/10/2015	206.29	2.35	-6.44
9/10/2015	207.77	2.37	-6.00
9/10/2015	207.77	2.37	-6.00
9/10/2015	208.62	2.40	0.23
9/10/2015	208.89	2.40	0.23
9/10/2015	208.77	2.40	3.17
9/10/2015	209.64	2.41	0.97
9/10/2015	208.66	2.41	6.37
9/10/2015	208.66	2.41	6.36
9/10/2015	210.67	2.43	10.14
9/10/2015	209.39	2.43	10.14
9/10/2015	210.92	2.42	1.70
9/10/2015	209.07	2.34	-25.43
9/10/2015	164.96	1.85	-24.91
9/10/2015	164.96	1.85	-24.89
9/10/2015	66.20	0.30	-134.67
9/10/2015	28.55	0.30	-134.67
9/10/2015	12.64	0.14	-88.51
9/10/2015	4.72	0.14	1167.61
9/10/2015	2.02	0.14	2987.20
9/10/2015	2.02	0.14	2987.26
9/10/2015	0.78	0.14	7462.69
9/10/2015	0.31	0.14	7462.69
9/10/2015	0.15	0.14	8462.21
9/10/2015	-0.26	0.14	12416.07

9/10/2015	-0.71	0.14	24016.35
9/10/2015	-0.71	0.14	24016.36
9/10/2015	-0.75	0.14	45257.47
9/10/2015	-0.95	0.14	45257.47
9/10/2015	-0.67	0.14	22298.05
9/10/2015	-0.39	0.14	14465.87
9/10/2015	-0.80	0.14	29531.79
9/10/2015	-0.80	0.14	29531.79
9/10/2015	-0.80	0.14	17338.61
9/10/2015	-0.52	0.14	17338.61
9/10/2015	-0.90	0.14	38814.99
9/10/2015	-0.29	0.14	12868.80
9/10/2015	16.74	0.14	-303.56
9/10/2015	16.74	0.14	-303.56
9/10/2015	55.53	0.76	-80.46
9/10/2015	70.89	0.76	-80.46
9/10/2015	78.09	0.87	-37.62
9/10/2015	82.72	0.93	-24.72
9/10/2015	84.70	0.97	-9.51
9/10/2015	84.70	0.97	-9.55
9/10/2015	84.84	0.99	-3.77
9/10/2015	85.93	0.99	-3.77
9/10/2015	86.36	1.00	-1.62
9/10/2015	86.73	1.00	-2.47
9/10/2015	86.57	1.00	1.75
9/10/2015	86.57	1.00	1.74
9/10/2015	86.64	1.01	10.47
9/10/2015	86.52	1.01	10.47
9/10/2015	86.51	1.01	6.80
9/10/2015	86.24	1.01	9.23
9/10/2015	86.72	1.00	1.12
9/10/2015	86.72	1.00	1.12
9/10/2015	86.84	1.01	1.19
9/10/2015	87.02	1.01	1.19
9/10/2015	86.81	1.01	4.33
9/10/2015	86.88	1.01	2.93
9/10/2015	85.96	1.01	11.59
9/10/2015	85.96	1.01	11.59
9/10/2015	85.94	1.00	6.88
9/10/2015	86.24	1.00	6.88
9/10/2015	86.97	1.01	4.61

9/10/2015	86.46	1.01	8.72
9/10/2015	87.09	1.01	-1.05
9/10/2015	87.09	1.01	-1.05
9/10/2015	87.38	1.01	2.06
9/10/2015	86.77	1.01	2.06
9/10/2015	86.60	1.00	2.22
9/10/2015	86.95	1.01	3.03
9/10/2015	86.78	1.01	5.66
9/10/2015	86.78	1.01	5.66
9/10/2015	87.05	1.01	-1.61
9/10/2015	87.52	1.01	-1.61
9/10/2015	87.46	1.02	3.90
9/10/2015	85.92	1.01	17.73
9/10/2015	86.88	1.01	1.17
9/10/2015	86.88	1.01	1.17
9/10/2015	86.97	1.01	3.59
9/10/2015	87.17	1.01	3.59
9/10/2015	86.74	1.01	5.31
9/10/2015	86.47	1.00	3.19
9/10/2015	87.22	1.01	-0.51
9/10/2015	87.22	1.01	-0.51
9/10/2015	87.21	1.01	6.23
9/10/2015	87.03	1.01	6.23
9/10/2015	86.98	1.01	4.75
9/10/2015	86.76	1.01	7.12
9/10/2015	86.81	1.01	4.49
9/10/2015	86.81	1.01	4.49
9/10/2015	86.81	1.01	13.58
9/10/2015	86.28	1.01	13.58
9/10/2015	86.63	1.01	3.86
9/10/2015	87.23	1.00	-4.35
9/10/2015	84.83	0.95	-35.39
9/10/2015	84.83	0.95	-35.39
9/10/2015	49.79	0.40	422.79
9/10/2015	23.78	0.40	422.79
9/10/2015	9.67	0.40	2304.96
9/10/2015	3.57	0.40	6546.87
9/10/2015	1.01	0.40	15178.24
9/10/2015	1.01	0.40	15178.28
9/10/2015	0.38	0.40	24849.14
9/10/2015	0.18	0.40	24849.14

9/10/2015	-0.73	0.40	71894.10
9/10/2015	-0.55	0.40	52906.15
9/10/2015	-0.87	0.40	100912.10
9/10/2015	-0.87	0.40	100912.11
9/10/2015	-0.37	0.40	102740.31
9/10/2015	-0.88	0.40	102740.31
9/10/2015	-0.31	0.40	38594.65
9/10/2015	-0.94	0.40	126200.94
9/10/2015	-1.01	0.40	166919.71
9/10/2015	-1.01	0.40	166919.71
9/10/2015	-0.63	0.40	152183.48
9/10/2015	-0.99	0.40	152183.48
9/10/2015	-0.25	0.40	35939.76
9/10/2015	-0.48	0.40	47562.26
9/10/2015	-0.66	0.40	63084.08
9/10/2015	-0.66	0.40	63084.08
9/10/2015	-0.84	0.40	238829.71
9/10/2015	-1.08	0.40	238829.71
9/10/2015	-0.34	0.40	40109.49
9/10/2015	-0.30	0.40	37980.71
9/10/2015	-0.92	0.40	115387.38
9/10/2015	-0.92	0.40	115387.37
9/10/2015	-1.06	0.40	55987.33
9/10/2015	-0.59	0.40	55987.33
9/10/2015	-0.53	0.40	50709.57
9/10/2015	-1.03	0.40	184062.40
9/10/2015	-0.87	0.40	99465.45
9/10/2015	-0.87	0.40	99465.45
9/10/2015	-0.69	0.40	127392.30
9/10/2015	-0.95	0.40	127392.30
9/10/2015	-0.60	0.40	56570.41
9/10/2015	-1.01	0.40	163338.66
9/10/2015	-1.06	0.40	220453.35
9/10/2015	-1.06	0.40	220453.35
9/10/2015	-0.52	0.40	95777.34
9/10/2015	-0.85	0.40	95777.34
9/10/2015	-0.69	0.40	65962.23
9/10/2015	-0.63	0.40	60148.68
9/10/2015	-0.93	0.40	121162.03
9/10/2015	-0.93	0.40	121162.02
9/10/2015	-1.03	0.40	106089.83

9/10/2015	-0.89	0.40	106089.83
9/10/2015	-0.68	0.40	65062.36
9/10/2015	-0.55	0.40	52338.32
9/10/2015	-1.11	0.40	309353.25
9/10/2015	-1.11	0.40	309353.26
9/10/2015	-0.60	0.40	94830.99
9/10/2015	-0.85	0.40	94830.99
9/10/2015	-1.12	0.40	319530.39
9/10/2015	-0.82	0.40	86987.10
9/10/2015	-0.22	0.40	35015.92
9/10/2015	-0.22	0.40	35015.92
9/10/2015	-1.09	0.40	340911.60
9/10/2015	-1.12	0.40	340911.60
9/10/2015	-1.04	0.40	195973.05
9/10/2015	-0.61	0.40	57551.35
9/10/2015	-1.08	0.40	246671.26
9/10/2015	-1.08	0.40	246671.26
9/10/2015	-1.01	0.40	52621.55
9/10/2015	-0.55	0.40	52621.55
9/10/2015	-0.82	0.40	87029.03
9/10/2015	-0.47	0.40	47081.64
9/10/2015	-0.70	0.40	67857.33
9/10/2015	-0.70	0.40	67857.33
9/10/2015	-0.95	0.40	62738.32
9/10/2015	-0.66	0.40	62738.32
9/10/2015	-1.07	0.40	228401.59
9/10/2015	-0.85	0.40	93963.54
9/10/2015	-0.29	0.40	37843.82
9/10/2015	-0.29	0.40	37843.83
9/10/2015	-1.01	0.40	40889.03
9/10/2015	-0.36	0.40	40889.03
9/10/2015	-0.84	0.40	92188.37
9/10/2015	-1.03	0.40	180182.35
9/10/2015	-0.41	0.40	43509.24
9/10/2015	-0.41	0.40	43509.24
9/10/2015	-0.75	0.40	67107.20
9/10/2015	-0.69	0.40	67107.20
9/10/2015	-1.13	0.40	352838.79
9/10/2015	-1.14	0.40	409775.17
9/10/2015	-0.55	0.40	52243.08
9/10/2015	-0.55	0.40	52243.08

9/10/2015	-1.11	0.40	258788.11
9/10/2015	-1.09	0.40	258788.11
9/10/2015	-0.63	0.40	59838.13
9/10/2015	-0.92	0.40	117806.05
9/10/2015	-1.06	0.40	216222.48
9/10/2015	-1.06	0.40	216222.48
9/10/2015	-0.60	0.40	196713.41
9/10/2015	-1.04	0.40	196713.41
9/10/2015	-0.77	0.40	77530.42
9/10/2015	-0.99	0.40	149882.82
9/10/2015	-1.03	0.40	182059.87
9/10/2015	-1.03	0.40	182059.86
9/10/2015	-1.16	0.40	78653.63
9/10/2015	-0.77	0.40	78653.63
9/10/2015	-0.44	0.40	45357.15
9/10/2015	-1.12	0.40	347941.58
9/10/2015	-1.11	0.40	302882.77
9/10/2015	-1.11	0.40	302882.77
9/10/2015	-0.85	0.40	85166.28
9/10/2015	-0.81	0.40	85166.28
9/10/2015	-0.94	0.40	125522.66
9/10/2015	-1.10	0.40	271194.53
9/10/2015	-0.92	0.40	117381.34
9/10/2015	-0.92	0.40	117381.34
9/10/2015	-0.35	0.40	190459.48
9/10/2015	-1.04	0.40	190459.48
9/10/2015	-0.88	0.40	103349.27
9/10/2015	-0.81	0.40	86278.89
9/10/2015	-0.49	0.40	48182.33
9/10/2015	-0.49	0.40	48182.33
9/10/2015	-0.99	0.40	69454.15
9/10/2015	-0.71	0.40	69454.15
9/10/2015	-0.68	0.40	65208.32
9/10/2015	-0.93	0.40	120931.98
9/10/2015	-0.58	0.40	55201.24
9/10/2015	-0.58	0.40	55201.24
9/10/2015	-0.20	0.40	49806.76
9/10/2015	-0.51	0.40	49806.76
9/10/2015	-0.56	0.40	53645.29
9/10/2015	-0.68	0.40	65174.07
9/10/2015	-0.68	0.40	64967.37

9/10/2015	-0.68	0.40	64967.37
9/10/2015	-1.09	0.40	119106.88
9/10/2015	-0.93	0.40	119106.88
9/10/2015	-0.62	0.40	58538.11
9/10/2015	-1.12	0.40	321136.05
9/10/2015	-0.94	0.40	126481.35
9/10/2015	-0.94	0.40	126481.35
9/10/2015	-0.86	0.40	417705.61
9/10/2015	-1.14	0.40	417705.61
9/10/2015	1722.62	19.82	7.91
9/10/2015	1722.62	19.82	7.87
9/10/2015	1730.20	19.79	3.80
9/10/2015	1726.49	19.79	3.80
9/10/2015	1726.73	19.75	1.66
9/10/2015	1728.33	19.74	0.15
9/10/2015	1729.51	19.74	-0.70
9/10/2015	1729.51	19.74	-0.71
9/10/2015	1732.50	19.73	-0.86
9/10/2015	1728.94	19.73	-0.86
9/10/2015	1731.37	19.71	-3.22
9/10/2015	1730.27	19.71	-2.68
9/10/2015	1728.50	19.69	-2.30
9/10/2015	1728.50	19.69	-2.31
9/10/2015	1734.72	19.72	-2.83
9/10/2015	1731.85	19.72	-2.83
9/10/2015	1729.48	19.69	-3.23
9/10/2015	1731.69	19.69	-4.56
9/10/2015	1731.28	19.69	-3.89
9/10/2015	1731.28	19.69	-3.90
9/10/2015	1734.65	19.71	-3.71
9/10/2015	1732.24	19.71	-3.71
9/10/2015	1730.79	19.69	-3.74
9/10/2015	1732.43	19.69	-4.60
9/10/2015	1731.96	19.70	-4.05
9/10/2015	1731.96	19.70	-4.05
9/10/2015	1736.59	19.72	-2.69
9/10/2015	1731.14	19.72	-2.69
9/10/2015	1732.42	19.69	-4.61
9/10/2015	1734.25	19.70	-5.22
9/10/2015	1731.37	19.70	-3.76
9/10/2015	1731.37	19.70	-3.77



9/10/2015	1733.89	19.68	-3.52
9/10/2015	1729.58	19.68	-3.52
9/10/2015	1730.18	19.66	-4.84
9/10/2015	1731.28	19.67	-5.10
9/10/2015	1733.12	19.68	-5.68
9/10/2015	1733.12	19.68	-5.68
9/10/2015	1735.80	19.70	-2.51
9/10/2015	1729.15	19.70	-2.51
9/10/2015	1733.18	19.68	-6.01
9/10/2015	1732.81	19.70	-4.75
9/10/2015	1731.77	19.69	-4.31
9/10/2015	1731.77	19.69	-4.32
9/10/2015	1733.83	19.68	-3.14
9/10/2015	1728.92	19.68	-3.14
9/10/2015	1731.41	19.67	-5.13
9/10/2015	1732.38	19.69	-4.93
9/10/2015	1729.20	19.68	-3.55
9/10/2015	1729.20	19.68	-3.56
9/10/2015	1737.70	18.40	-40.70
9/10/2015	1677.21	18.40	-40.70
9/10/2015	1248.90	13.80	-33.52
9/10/2015	648.61	7.50	12.38
9/10/2015	289.21	3.06	-78.81
9/10/2015	289.21	3.06	-78.74
9/10/2015	91.78	-0.03	-1095.38
9/10/2015	42.55	-0.03	-1095.38
9/10/2015	22.45	-0.17	-1672.75
9/10/2015	13.33	-0.17	-2074.32
9/10/2015	8.42	-0.17	-2605.95
9/10/2015	8.42	-0.17	-2605.74
9/10/2015	6.20	-0.17	-3567.65
9/10/2015	4.76	-0.17	-3567.65
9/10/2015	4.17	-0.17	-3844.15
9/10/2015	4.30	-0.17	-3779.15
9/10/2015	3.12	-0.17	-4519.85
9/10/2015	3.12	-0.17	-4519.82
9/10/2015	2.53	-0.17	-4855.01
9/10/2015	2.74	-0.17	-4855.01
9/10/2015	2.68	-0.17	-4912.06
9/10/2015	2.35	-0.17	-5276.85
9/10/2015	2.46	-0.17	-5144.66

9/10/2015	2.18	-0.17	-7913.21
9/10/2015	0.98	-0.17	-7913.21
9/10/2015	1.29	-0.17	-7062.95
9/10/2015	1.62	-0.17	-6366.89
9/10/2015	0.57	-0.17	-9461.31
9/10/2015	0.57	-0.17	-9461.30
9/10/2015	1.33	-0.17	-6838.69
9/10/2015	1.39	-0.17	-6838.69
9/10/2015	0.82	-0.17	-8454.34
9/10/2015	0.61	-0.17	-9277.36
9/10/2015	0.88	-0.17	-8226.11
9/10/2015	0.88	-0.17	-8226.11
9/10/2015	0.72	-0.17	-10890.39
9/10/2015	0.31	-0.17	-10890.39
9/10/2015	1.12	-0.17	-7488.16
9/10/2015	0.64	-0.17	-9142.43
9/10/2015	0.06	-0.17	-12769.82
9/10/2015	0.06	-0.17	-12769.81
9/10/2015	1.07	-0.17	-11480.11
9/10/2015	0.22	-0.17	-11480.11
9/10/2015	0.25	-0.17	-11327.48
9/10/2015	-0.08	-0.17	-14275.44
9/10/2015	0.39	-0.17	-10441.54
9/10/2015	0.39	-0.17	-10441.54
9/10/2015	0.34	-0.17	-14289.23
9/10/2015	-0.08	-0.17	-14289.23
9/10/2015	-0.38	-0.17	-18834.74
9/10/2015	0.12	-0.17	-12306.13
9/10/2015	0.58	-0.17	-9415.95
9/10/2015	0.58	-0.17	-9415.95
9/10/2015	0.30	-0.17	-11526.88
9/10/2015	0.22	-0.17	-11526.88
9/10/2015	-0.39	-0.17	-19167.96
9/10/2015	0.14	-0.17	-12123.08
9/10/2015	-0.71	-0.17	-30153.22
9/10/2015	-0.71	-0.17	-30153.22
9/10/2015	0.52	-0.17	-11650.56
9/10/2015	0.20	-0.17	-11650.56
9/10/2015	-0.36	-0.17	-18525.23
9/10/2015	-0.14	-0.17	-15027.96
9/10/2015	-0.01	-0.17	-13512.32

9/10/2015	-0.01	-0.17	-13512.32
9/10/2015	0.05	-0.17	-13285.22
9/10/2015	0.01	-0.17	-13285.22
9/10/2015	-0.46	-0.17	-20748.74
9/10/2015	-0.41	-0.17	-19682.67
9/10/2015	-0.54	-0.17	-23130.51
9/10/2015	-0.54	-0.17	-23130.51
9/10/2015	-0.57	-0.17	-30691.65
9/10/2015	-0.72	-0.17	-30691.65
9/10/2015	0.01	-0.17	-13245.53
9/10/2015	-0.18	-0.17	-15531.99
9/10/2015	-0.63	-0.17	-26442.39
9/10/2015	-0.63	-0.17	-26442.39
9/10/2015	-0.07	-0.17	-22905.62
9/10/2015	-0.53	-0.17	-22905.62
9/10/2015	-0.45	-0.17	-20520.89
9/10/2015	-0.77	-0.17	-34208.53
9/10/2015	-0.93	-0.17	-52013.84
9/10/2015	-0.93	-0.17	-52013.83
9/10/2015	-0.79	-0.17	-16260.95
9/10/2015	-0.23	-0.17	-16260.95
9/10/2015	-0.07	-0.17	-14184.51
9/10/2015	-0.32	-0.17	-17763.94
9/10/2015	-0.21	-0.17	-15936.93
9/10/2015	-0.21	-0.17	-15936.93
9/10/2015	-0.77	-0.17	-25447.69
9/10/2015	-0.61	-0.17	-25447.69
9/10/2015	-0.75	-0.17	-32868.55
9/10/2015	-1.03	-0.17	-76343.73
9/10/2015	-0.53	-0.17	-22721.82
9/10/2015	-0.53	-0.17	-22721.82
9/10/2015	-0.80	-0.17	-37584.58
9/10/2015	-0.81	-0.17	-37584.58
9/10/2015	-0.61	-0.17	-25526.81
9/10/2015	-0.23	-0.17	-16263.48
9/10/2015	-0.37	-0.17	-18780.86
9/10/2015	-0.37	-0.17	-18780.87
9/10/2015	-0.93	-0.17	-23179.30
9/10/2015	-0.54	-0.17	-23179.30
9/10/2015	-0.35	-0.17	-18247.27
9/10/2015	-0.30	-0.17	-17330.66

9/10/2015	-0.39	-0.17	-19067.12
9/10/2015	-0.39	-0.17	-19067.12
9/10/2015	-0.69	-0.17	-17809.38
9/10/2015	-0.32	-0.17	-17809.38
9/10/2015	-0.16	-0.17	-15175.67
9/10/2015	-0.74	-0.17	-32241.74
9/10/2015	-0.11	-0.17	-14630.06
9/10/2015	-0.11	-0.17	-14630.06
9/10/2015	-0.31	-0.17	-45455.10
9/10/2015	-0.89	-0.17	-45455.10
9/10/2015	-0.16	-0.17	-15276.19
9/10/2015	-0.91	-0.17	-48073.80
9/10/2015	-0.91	-0.17	-49308.93
9/10/2015	-0.91	-0.17	-49308.93
9/10/2015	-0.57	-0.17	-19416.19
9/10/2015	-0.40	-0.17	-19416.19
9/10/2015	-0.40	-0.17	-19256.06
9/10/2015	-0.98	-0.17	-63314.55
9/10/2015	-0.37	-0.17	-18678.92
9/10/2015	-0.37	-0.17	-18678.93
9/10/2015	-0.62	-0.17	-50875.08
9/10/2015	-0.92	-0.17	-50875.08
9/10/2015	-0.08	-0.17	-14297.56
9/10/2015	-0.92	-0.17	-50508.42
9/10/2015	-0.97	-0.17	-60117.34
9/10/2015	-0.97	-0.17	-60117.34
9/10/2015	-0.13	-0.17	-19182.53
9/10/2015	-0.39	-0.17	-19182.53
9/10/2015	-0.51	-0.17	-22148.39
9/10/2015	-0.21	-0.17	-15990.09
9/10/2015	-0.72	-0.17	-31069.76
9/10/2015	-0.72	-0.17	-31069.75
9/10/2015	-1.05	-0.17	-43632.44
9/10/2015	-0.87	-0.17	-43632.44
9/10/2015	-0.39	-0.17	-19181.45
9/10/2015	-0.06	-0.17	-14018.94
9/10/2015	-0.59	-0.17	-24639.52
9/10/2015	-0.59	-0.17	-24639.53
9/10/2015	-0.85	-0.17	-70793.80
9/10/2015	-1.01	-0.17	-70793.80

Table 2. UtPtP-C-3-flbk 3 071415 flowback fluid raw data for DOC analysis where “sniff” and “pulse” peaks are indentified.

	UtPtP-C-3-flbk 3 071415		
DATE	12CO2	13CO2_Raw	Delta_Raw
1/26/2016	2.3613	2.91E-01	913.7506
1/26/2016	12.3036	2.91E-01	913.7506
1/26/2016	13.2506	2.91E-01	786.5500
1/26/2016	10.0865	2.91E-01	1294.8013
1/26/2016	8.1010	2.91E-01	1789.7727
1/26/2016	8.1010	2.91E-01	1789.7370
1/26/2016	7.5780	2.91E-01	1803.4575
1/26/2016	8.0559	2.91E-01	1803.4575
1/26/2016	7.2919	2.91E-01	2057.6128
1/26/2016	8.4092	2.91E-01	1699.5437
1/26/2016	7.5116	2.91E-01	1979.9442
1/26/2016	7.5116	2.91E-01	1979.9464
1/26/2016	7.4626	2.91E-01	1956.4861
1/26/2016	7.5803	2.91E-01	1956.4861
1/26/2016	7.0528	2.91E-01	2146.7869
1/26/2016	7.2274	2.91E-01	2081.1467
1/26/2016	7.2500	2.91E-01	2072.8763
1/26/2016	7.2500	2.91E-01	2072.8754
1/26/2016	7.0527	2.91E-01	2100.0802
1/26/2016	7.1763	2.91E-01	2100.0802
1/26/2016	8.0715	2.91E-01	1798.7035
1/26/2016	7.0241	2.91E-01	2157.8349
1/26/2016	7.2526	2.91E-01	2071.9229
1/26/2016	7.2526	2.91E-01	2071.9247
1/26/2016	4.8019	2.91E-01	10773.3542
1/26/2016	1.0008	2.91E-01	10773.3542
1/26/2016	-0.0650	2.91E-01	21584.1706
1/26/2016	-0.7181	2.91E-01	50514.3253
1/26/2016	-0.8586	2.91E-01	70081.4401
1/26/2016	-0.8586	2.91E-01	70081.4645
1/26/2016	-1.1221	2.91E-01	378916.1608
1/26/2016	-1.1594	2.91E-01	378916.1608
1/26/2016	-0.8914	2.91E-01	76994.9096
1/26/2016	-0.9822	2.91E-01	105723.6484
1/26/2016	-0.9360	2.91E-01	88892.1814
1/26/2016	-0.9360	2.91E-01	88892.1869
1/26/2016	-0.8830	2.91E-01	392225.9322

1/26/2016	-1.1617	2.91E-01	392225.9322
1/26/2016	-0.4511	2.91E-01	32814.4842
1/26/2016	-1.0885	2.91E-01	186744.5425
1/26/2016	-0.7750	2.91E-01	56977.3588
1/26/2016	-0.7750	2.91E-01	56977.3557
1/26/2016	-0.9146	2.91E-01	46258.4601
1/26/2016	-0.6722	2.91E-01	46258.4601
1/26/2016	-1.1551	2.91E-01	356640.7928
1/26/2016	-1.1525	2.91E-01	344352.8784
1/26/2016	3.5553	2.91E-01	4470.0263
1/26/2016	3.5553	2.91E-01	4470.0089
1/26/2016	20.0624	2.91E-01	-81.4766
1/26/2016	26.4862	2.91E-01	-81.4766
1/26/2016	29.6646	2.67E-01	-249.7311
1/26/2016	30.4216	2.57E-01	-297.9427
1/26/2016	30.8821	2.86E-01	-224.7960
1/26/2016	30.8821	2.86E-01	-224.8765
1/26/2016	30.8259	3.10E-01	-142.6530
1/26/2016	30.2823	3.10E-01	-142.6530
1/26/2016	31.2397	3.21E-01	-136.6633
1/26/2016	31.2446	3.31E-01	-108.5913
1/26/2016	31.2034	3.36E-01	-94.9001
1/26/2016	31.2034	3.36E-01	-94.9035
1/26/2016	30.9025	3.43E-01	-81.1620
1/26/2016	31.4524	3.43E-01	-81.1620
1/26/2016	30.5466	3.44E-01	-51.7688
1/26/2016	30.7227	3.42E-01	-63.9898
1/26/2016	30.5296	3.45E-01	-47.8737
1/26/2016	30.5296	3.45E-01	-47.8779
1/26/2016	31.1291	3.52E-01	-59.6855
1/26/2016	31.5480	3.52E-01	-59.6855
1/26/2016	30.5244	3.50E-01	-33.5179
1/26/2016	30.5278	3.46E-01	-44.8180
1/26/2016	30.9067	3.49E-01	-50.1904
1/26/2016	30.9067	3.49E-01	-50.1890
1/26/2016	30.9671	3.52E-01	-30.6440
1/26/2016	30.5632	3.52E-01	-30.6440
1/26/2016	30.8836	3.53E-01	-36.4477
1/26/2016	30.9353	3.55E-01	-32.2611
1/26/2016	31.2174	3.53E-01	-47.8591
1/26/2016	31.2174	3.53E-01	-47.8627

1/26/2016	31.4241	3.56E-01	-44.4172
1/26/2016	31.4117	3.56E-01	-44.4172
1/26/2016	31.3106	3.58E-01	-36.8002
1/26/2016	30.8772	3.53E-01	-35.8042
1/26/2016	30.7161	3.51E-01	-38.3159
1/26/2016	30.7161	3.51E-01	-38.3193
1/26/2016	31.9746	3.60E-01	-45.8747
1/26/2016	31.7789	3.60E-01	-45.8747
1/26/2016	31.8544	3.55E-01	-59.4579
1/26/2016	31.8344	3.59E-01	-50.0293
1/26/2016	31.6249	3.61E-01	-38.0200
1/26/2016	31.6249	3.61E-01	-38.0210
1/26/2016	32.2268	3.59E-01	-40.0646
1/26/2016	31.5391	3.59E-01	-40.0646
1/26/2016	30.9767	3.58E-01	-25.7106
1/26/2016	31.2818	3.60E-01	-29.5349
1/26/2016	30.7402	3.57E-01	-21.2594
1/26/2016	30.7402	3.57E-01	-21.2575
1/26/2016	31.0496	3.51E-01	-49.7714
1/26/2016	31.0952	3.51E-01	-49.7714
1/26/2016	31.0668	3.48E-01	-57.4374
1/26/2016	31.8012	3.53E-01	-66.0228
1/26/2016	31.6776	3.60E-01	-41.1878
1/26/2016	31.6776	3.60E-01	-41.1899
1/26/2016	32.2874	3.63E-01	-46.7030
1/26/2016	32.0903	3.63E-01	-46.7030
1/26/2016	31.2497	3.61E-01	-25.8885
1/26/2016	30.2052	3.48E-01	-28.6115
1/26/2016	30.7642	3.53E-01	-32.4188
1/26/2016	30.7642	3.53E-01	-32.4331
1/26/2016	50.3703	6.20E-01	-102.2479
1/26/2016	59.1094	6.20E-01	-102.2479
1/26/2016	32.9646	4.00E-01	26.2009
1/26/2016	13.7767	2.45E-01	443.9315
1/26/2016	5.8414	2.45E-01	2099.5367
1/26/2016	5.8414	2.45E-01	2099.6145
1/26/2016	1.0495	2.45E-01	22061.7260
1/26/2016	-0.2702	2.45E-01	22061.7260
1/26/2016	-0.3322	2.45E-01	23660.0306
1/26/2016	-1.1110	2.45E-01	187072.0970
1/26/2016	-0.7862	2.45E-01	48990.8530

1/26/2016	-0.7862	2.45E-01	48990.8924
1/26/2016	-1.0032	2.45E-01	119733.3231
1/26/2016	-1.0454	2.45E-01	119733.3231
1/26/2016	-0.6147	2.45E-01	35019.3420
1/26/2016	-0.7386	2.45E-01	44133.6554
1/26/2016	-0.4559	2.45E-01	27612.4066
1/26/2016	-0.4559	2.45E-01	27612.4128
1/26/2016	-0.8676	2.45E-01	23059.5907
1/26/2016	-0.3099	2.45E-01	23059.5907
1/26/2016	-0.4345	2.45E-01	26839.0614
1/26/2016	-0.8122	2.45E-01	52118.2189
1/26/2016	-0.8151	2.45E-01	52487.5309
1/26/2016	-0.8151	2.45E-01	52487.5320
1/26/2016	-0.7765	2.45E-01	44291.9841
1/26/2016	-0.7403	2.45E-01	44291.9841
1/26/2016	-1.1549	2.45E-01	299150.0939
1/26/2016	-1.0630	2.45E-01	132564.1502
1/26/2016	-1.1591	2.45E-01	317259.6884
1/26/2016	-1.1591	2.45E-01	317259.6932
1/26/2016	-1.0974	2.45E-01	40116.4292
1/26/2016	-0.6907	2.45E-01	40116.4292
1/26/2016	-0.2384	2.45E-01	21321.2633
1/26/2016	-0.8520	2.45E-01	57728.0611
1/26/2016	-0.1079	2.45E-01	18718.2737
1/26/2016	-0.1079	2.45E-01	18718.2734
1/26/2016	-0.6624	2.45E-01	187796.6143
1/26/2016	-1.1115	2.45E-01	187796.6143
1/26/2016	-0.7679	2.45E-01	47003.4805
1/26/2016	-0.8756	2.45E-01	61665.7162
1/26/2016	-1.1094	2.45E-01	184487.7063
1/26/2016	-1.1094	2.45E-01	184487.7052
1/26/2016	-1.1186	2.45E-01	205226.9486
1/26/2016	-1.1214	2.45E-01	205226.9486
1/26/2016	-0.7291	2.45E-01	43274.8343
1/26/2016	-0.9326	2.45E-01	73728.0582
1/26/2016	-0.8270	2.45E-01	54073.2664
1/26/2016	-0.8270	2.45E-01	54073.2697
1/26/2016	-1.1755	2.45E-01	200441.4219
1/26/2016	-1.1188	2.45E-01	200441.4219
1/26/2016	-1.1687	2.45E-01	368052.2228
1/26/2016	-0.7989	2.45E-01	50467.0154



1/26/2016	-0.8344	2.45E-01	55102.5214
1/26/2016	-0.8344	2.45E-01	55102.5218
1/26/2016	-0.9280	2.45E-01	129634.8759
1/26/2016	-1.0593	2.45E-01	129634.8759
1/26/2016	-1.1703	2.45E-01	378180.6419
1/26/2016	-0.6466	2.45E-01	36992.4662
1/26/2016	-1.1548	2.45E-01	298595.0731
1/26/2016	-1.1548	2.45E-01	298595.0706
1/26/2016	-1.0993	2.45E-01	43495.7549
1/26/2016	-0.7316	2.45E-01	43495.7549
1/26/2016	-1.0152	2.45E-01	102660.9348
1/26/2016	-0.9976	2.45E-01	94773.0494
1/26/2016	-1.1736	2.45E-01	400822.4235
1/26/2016	-1.1736	2.45E-01	400822.4250
1/26/2016	-1.1007	2.45E-01	91928.5615
1/26/2016	-0.9906	2.45E-01	91928.5615
1/26/2016	-0.9247	2.45E-01	71780.4799
1/26/2016	-1.1316	2.45E-01	226930.8621
1/26/2016	-0.9773	2.45E-01	87029.9235
1/26/2016	-0.9773	2.45E-01	87029.9245
1/26/2016	-0.7027	2.45E-01	41694.2863
1/26/2016	-0.7106	2.45E-01	41694.2863
1/26/2016	-0.8283	2.45E-01	54254.0428
1/26/2016	-1.1097	2.45E-01	184993.6264
1/26/2016	-0.8455	2.45E-01	56730.6106
1/26/2016	-0.8455	2.45E-01	56730.6094
1/26/2016	-0.8045	2.45E-01	56498.8428
1/26/2016	-0.8439	2.45E-01	56498.8428
1/26/2016	-0.6640	2.45E-01	38164.8440
1/26/2016	-0.2189	2.45E-01	20888.2842
1/26/2016	-1.0998	2.45E-01	170661.5744
1/26/2016	-1.0998	2.45E-01	170661.5750
1/26/2016	-0.8542	2.45E-01	201814.8514
1/26/2016	-1.1196	2.45E-01	201814.8514
1/26/2016	-1.1031	2.45E-01	175224.9425
1/26/2016	-0.6740	2.45E-01	38870.9848
1/26/2016	-0.7402	2.45E-01	44284.2816
1/26/2016	-0.7402	2.45E-01	44284.2817
1/26/2016	-0.6744	2.45E-01	43903.5420
1/26/2016	-0.7361	2.45E-01	43903.5420
1/26/2016	-0.6681	2.45E-01	38453.8627

1/26/2016	-1.1197	2.45E-01	202051.4758
1/26/2016	-1.1640	2.45E-01	341220.9619
1/26/2016	-1.1640	2.45E-01	341220.9596
1/26/2016	-0.3214	2.45E-01	39095.7796
1/26/2016	-0.6771	2.45E-01	39095.7796
1/26/2016	-0.5092	2.45E-01	29734.6045
1/26/2016	-0.9562	2.45E-01	80209.9476
1/26/2016	-0.8110	2.45E-01	51961.9799
1/26/2016	-0.8110	2.45E-01	51961.9802
1/26/2016	-0.8932	2.45E-01	162557.6034
1/26/2016	-1.0934	2.45E-01	162557.6034
1/26/2016	-1.1343	2.45E-01	233460.8973
1/26/2016	-1.0636	2.45E-01	133040.1087
1/26/2016	-0.9490	2.45E-01	78116.3866
1/26/2016	-0.9490	2.45E-01	78116.3880
1/26/2016	-1.1156	2.45E-01	152682.6458
1/26/2016	-1.0847	2.45E-01	152682.6458
1/26/2016	-0.9331	2.45E-01	73843.3679
1/26/2016	-0.8521	2.45E-01	57751.8565
1/26/2016	-0.9357	2.45E-01	74519.4952
1/26/2016	-0.9357	2.45E-01	74519.4944
1/26/2016	-1.1378	2.45E-01	21981.2659
1/26/2016	-0.2668	2.45E-01	21981.2659
1/26/2016	-1.1209	2.45E-01	204290.5064
1/26/2016	-0.6985	2.45E-01	40718.9931
1/26/2016	-1.1781	2.45E-01	436428.3531
1/26/2016	-1.1781	2.45E-01	436428.3548
1/26/2016	-1.0348	2.45E-01	209571.0827
1/26/2016	-1.1236	2.45E-01	209571.0827
1/26/2016	-0.8768	2.45E-01	61868.1424
1/26/2016	-1.3100	2.45E-01	-273344.6498
1/26/2016	-0.8796	2.45E-01	62377.8391
1/26/2016	-0.8796	2.45E-01	62377.8379
1/26/2016	-0.7363	2.45E-01	1697668.5740
1/26/2016	-1.2156	2.45E-01	1697668.5740
1/26/2016	-0.7749	2.45E-01	47748.1164
1/26/2016	-1.1150	2.45E-01	193611.8662
1/26/2016	-0.7165	2.45E-01	42181.4999
1/26/2016	-0.7165	2.45E-01	42181.4994
1/26/2016	-1.0187	2.45E-01	177136.9012
1/26/2016	-1.1044	2.45E-01	177136.9012

1/26/2016	-0.7560	2.45E-01	45800.7571
1/26/2016	-1.0632	2.45E-01	132724.9113
1/26/2016	-0.6739	2.45E-01	38867.0449
1/26/2016	-0.6739	2.45E-01	38867.0455
1/26/2016	-1.1468	2.45E-01	60217.9639
1/26/2016	-0.8673	2.45E-01	60217.9639
1/26/2016	-1.1309	2.45E-01	225344.2942
1/26/2016	-0.7689	2.45E-01	47114.5981
1/26/2016	-0.9056	2.45E-01	67478.3841
1/26/2016	-0.9056	2.45E-01	67478.3853
1/26/2016	-1.2833	2.45E-01	116764.0046
1/26/2016	-1.0408	2.45E-01	116764.0046
1/26/2016	-1.1007	2.45E-01	171999.0352
1/26/2016	-1.1697	2.45E-01	374303.8348
1/26/2016	-0.8229	2.45E-01	53518.3412
1/26/2016	-0.8229	2.45E-01	53518.3416
1/26/2016	-1.0445	2.45E-01	32639.5779
1/26/2016	-0.5713	2.45E-01	32639.5779
1/26/2016	-1.0721	2.45E-01	140328.6428
1/26/2016	-0.7603	2.45E-01	46223.9015
1/26/2016	-0.6359	2.45E-01	36310.6981
1/26/2016	-0.6359	2.45E-01	36310.6980
1/26/2016	-1.0030	2.45E-01	51156.9707
1/26/2016	-0.8045	2.45E-01	51156.9707
1/26/2016	0.1612	2.45E-01	14894.6464
1/26/2016	-1.0628	2.45E-01	132401.6981
1/26/2016	-0.1766	2.45E-01	20007.2067
1/26/2016	-0.1766	2.45E-01	20007.2088
1/26/2016	-1.1698	2.45E-01	180864.3442
1/26/2016	-1.1070	2.45E-01	180864.3442
1/26/2016	-1.0078	2.45E-01	99193.0508
1/26/2016	-1.1218	2.45E-01	205989.4677
1/26/2016	-1.0034	2.45E-01	97231.6781
1/26/2016	-1.0034	2.45E-01	97231.6739
1/26/2016	-0.9822	2.45E-01	133732.9404
1/26/2016	-1.0644	2.45E-01	133732.9404
1/26/2016	-0.3146	2.45E-01	23183.9109
1/26/2016	-1.1168	2.45E-01	196843.7118
1/26/2016	-1.0067	2.45E-01	98702.1939
1/26/2016	-1.0067	2.45E-01	98702.1946
1/26/2016	-0.8795	2.45E-01	69124.1202

1/26/2016	-0.9132	2.45E-01	69124.1202
1/26/2016	-1.1407	2.45E-01	250456.8013
1/26/2016	-1.1556	2.45E-01	301702.5726
1/26/2016	-1.1272	2.45E-01	217093.9008
1/26/2016	-1.1272	2.45E-01	217093.9017
1/26/2016	-1.1256	2.45E-01	58706.1803
1/26/2016	-0.8581	2.45E-01	58706.1803
1/26/2016	-0.6567	2.45E-01	37663.7703
1/26/2016	-1.1184	2.45E-01	199742.5376
1/26/2016	-0.6616	2.45E-01	37999.0648
1/26/2016	-0.6616	2.45E-01	37999.0653
1/26/2016	-1.1587	2.45E-01	33401.5573
1/26/2016	-0.5858	2.45E-01	33401.5573
1/26/2016	-1.1617	2.45E-01	329254.2922
1/26/2016	0.2892	2.45E-01	13551.3812
1/26/2016	-1.0198	2.45E-01	104957.7751
1/26/2016	-1.0198	2.45E-01	104957.7752
1/26/2016	-1.1700	2.45E-01	403794.1970
1/26/2016	-1.1740	2.45E-01	403794.1970
1/26/2016	-0.7736	2.45E-01	47611.7219
1/26/2016	-0.7029	2.45E-01	41067.5228
1/26/2016	-1.0018	2.45E-01	96519.8516
1/26/2016	-1.0018	2.45E-01	96519.8521
1/26/2016	-1.0463	2.45E-01	22076.0211
1/26/2016	-0.2708	2.45E-01	22076.0211
1/26/2016	-1.1312	2.45E-01	226015.8951
1/26/2016	-1.0027	2.45E-01	96941.2087
1/26/2016	-0.8741	2.45E-01	61393.6030
1/26/2016	-0.8741	2.45E-01	61393.6030
1/26/2016	-1.0643	2.45E-01	827794.8386
1/26/2016	-1.2020	2.45E-01	827794.8386
1/26/2016	-0.7242	2.45E-01	42845.5613
1/26/2016	-0.9850	2.45E-01	89797.4804
1/26/2016	-1.1208	2.45E-01	204184.7706
1/26/2016	-1.1208	2.45E-01	204184.7678
1/26/2016	-0.9224	2.45E-01	97877.3948
1/26/2016	-1.0049	2.45E-01	97877.3948
1/26/2016	-1.1306	2.45E-01	224661.5697
1/26/2016	-1.0026	2.45E-01	96895.7324
1/26/2016	-0.6690	2.45E-01	38516.7846
1/26/2016	-0.6690	2.45E-01	38516.7884

1/26/2016	-1.1788	2.45E-01	60830.7108
1/26/2016	-0.8709	2.45E-01	60830.7108
1/26/2016	-1.0981	2.45E-01	168510.4187
1/26/2016	-1.1125	2.45E-01	189526.5427
1/26/2016	-0.8371	2.45E-01	55498.1331
1/26/2016	-0.8371	2.45E-01	55498.1307
1/26/2016	-0.8636	2.45E-01	98991.3894
1/26/2016	-1.0074	2.45E-01	98991.3894
1/26/2016	-0.7857	2.45E-01	48938.3520
1/26/2016	-0.5816	2.45E-01	33173.8030